

A higher order pressure-stabilized virtual element formulation for the Stokes–Poisson–Boltzmann equations

Sudheer Mishra^a, Sundararajan Natarajan^a, E. Natarajan^b, and Gianmarco Manzini^c

^a*Department of Mechanical Engineering, Indian Institute of Technology Madras, Chennai 600036, India*

^b*Department of Mathematics, Indian Institute of Space Science and Technology, Thiruvananthapuram 695547, India*

^c*Istituto di Matematica Applicata e Tecnologie Informatiche Consiglio Nazionale delle Ricerche, Pavia 27100, Italy*

Abstract

Electrokinetic phenomena in nanopore sensors and microfluidic devices require accurate simulation of coupled fluid-electrostatic interactions in geometrically complex domains with irregular boundaries and adaptive mesh refinement. We develop an equal-order virtual element method for the Stokes–Poisson–Boltzmann equations that naturally handles general polygonal meshes, including meshes with hanging nodes, without requiring special treatment or remeshing. The key innovation is a residual-based pressure stabilization scheme derived by reformulating the Laplacian drag force in the momentum equation as a weighted advection term involving the nonlinear Poisson–Boltzmann equation, thereby eliminating second-order derivative terms while maintaining theoretical rigor. Well-posedness of the coupled stabilized problem is established using the Banach and Brouwer fixed-point theorems under sufficiently small data assumptions, and optimal a priori error estimates are derived in the energy norm with convergence rates of order $\mathcal{O}(h^k)$ for approximation degree $k \geq 1$. Numerical experiments on diverse polygonal meshes—including distorted elements, non-convex polygons, Voronoi tessellations, and configurations with hanging nodes—confirm optimal convergence rates, validating theoretical predictions. Applications to electro-osmotic flows in nanopore sensors with complex obstacle geometries illustrate the method’s practical utility for engineering simulations. Compared to Taylor–Hood finite element formulations, the equal-order approach simplifies implementation through uniform polynomial treatment of all fields and offers native support for general polygonal elements.

Keywords: Stokes–Poisson–Boltzmann equation, Virtual element method, Equal-order approximation, Pressure stabilization, Polygonal meshes, Electrokinetic flows, Nanopore sensors
Mathematics Subject Classification: 65N12, 65N30, 76D07

1. Introduction

Nanopore sensors have emerged as transformative tools for single-molecule analysis, DNA sequencing, and ion channel studies [1]. The fundamental physics governing these devices involves coupled fluid-electrostatic interactions: ionic transport through nanoscale pores is driven by both pressure gradients and applied electric fields, while electrostatic potentials arise from charge distributions in thin electrical double layers near solid boundaries. Accurate numerical simulation of these electrokinetic phenomena requires solving the Stokes equations coupled with the Poisson–Boltzmann equation, and the geometric complexity of realistic nanopore structures—including irregular pore shapes, multiple obstacles, and interfaces requiring adaptive mesh refinement—poses significant challenges for conventional numerical methods.

Standard finite element methods (FEM) for the Stokes–Poisson–Boltzmann (SPB) system typically employ mixed approximation spaces to satisfy the discrete inf-sup condition. For instance,

Taylor-Hood $\mathbb{P}_{k+1}/\mathbb{P}_k$ elements [2] use higher-order velocity approximations to ensure stability. While theoretically sound, these approaches face practical limitations: (i) implementation complexity of mixed finite element spaces with different approximation orders, (ii) difficulty handling hanging nodes arising from adaptive mesh refinement, and (iii) restricted mesh flexibility when approximating domains with irregular boundaries. Virtual element methods (VEM) offer an attractive alternative by enabling equal-order approximations on general polygonal meshes, with a projection-based framework that naturally handles arbitrary element shapes and hanging nodes.

Recent work by AlSohaim, Ruiz-Baier, and Villa-Fuentes [2] developed a finite element formulation for the SPB system using Taylor-Hood spaces on triangular meshes, establishing theoretical foundations through fixed-point analysis and deriving optimal error estimates. While this work provides important theoretical results, the geometric constraints of conforming triangular meshes and the complexity of mixed-order implementations motivate exploration of alternative approaches. In particular, equal-order approximations and the polytopal flexibility offered by VEM remain unexplored for this problem class.

Electrokinetic phenomena in charged fluids play a significant role in micro-scale and nano-scale transport processes [3, 4, 5], with applications spanning nanopore design for DNA sequencing, ion transport modeling in water purification systems [6], and microfluidic device development [7]. Among these, electro-osmotic flow—arising from the interaction between an externally applied electric field and charged species within thin electric double layers—represents one of the most efficient mechanisms for inducing fluid motion without mechanical actuation. In this work, fluid motion is modeled using the Stokes equations with a forcing term dependent on the electrolyte charge and the applied electric field. The fluid velocities considered are not sufficiently strong to affect the electrostatic potential distribution within the double layer; consequently, the electric charge density can be directly related to the potential through the Poisson-Boltzmann equation, supplemented by an advection term coupling the fluid velocity and potential.

Concerning the Poisson-Boltzmann equation (PBE), finite element formulations have been discussed in [8, 9, 10], with extension to general polygons in [11]. Following [2], we consider the regularized form of this equation, which preserves the nonlinearity characterized by a hyperbolic sine function but omits the distributional Dirac forcing term. We also incorporate the convection term coupling fluid velocity and potential, and impose a restriction on the functional space requiring the double layer potential field to be bounded as discussed in [10].

Polytopal methods have attracted considerable attention because they provide flexibility in dealing with complex geometries and irregular interfaces, where standard methods like FEM or the finite difference method (FDM) might be computationally costly. To address the challenge that extending FEM to polytopal meshes requires explicit construction of shape functions, Beirão da Veiga et al. [12] introduced the virtual element method (VEM), which handles arbitrary polygonal/polyhedral meshes without explicit basis function formulation. Instead, VEM requires only suitable choices of degrees of freedom to compute the discrete formulation, enabling easy extension to higher-order approximations while maintaining robustness under general mesh types. VEM has been applied to elasticity [13, 14], Oseen problem [15, 16], Stokes and Navier-Stokes problems [17, 18, 19, 20, 21, 22], Maxwell equation [23], plate bending [24], crack propagation [25, 26], optimization [27, 28], and magnetostatics [29]. For the Stokes problem, Guo and Feng [30] introduced a projection-based stabilized VEM using equal-order velocity-pressure pairs, circumventing the discrete inf-sup condition without requiring second-order derivative terms or coupling terms. This approach has been extended to the unsteady Navier-Stokes equations [31], the Oseen problem [32], and coupled problems including Stokes-Darcy [33] and Stokes-Temperature [34].

While VEM has been successfully applied to various coupled multiphysics problems including Stokes-Darcy flows, Navier-Stokes equations coupled with temperature, and fluid-structure interac-

tion, its application to electrokinetic systems described by the SPB equations remains unexplored. The SPB coupling introduces specific challenges distinct from previously studied systems: (i) the nonlinearity through the hyperbolic sine term $\kappa(\psi) = \alpha_0 \sinh(\alpha_1 \psi)$ requires careful fixed-point analysis; (ii) the potential-dependent drag forces in the momentum equation couple velocity gradients with electrostatic gradients; (iii) the strong interaction between pressure gradients and electrostatic forces necessitates robust stabilization strategies. These features distinguish the SPB system from standard Stokes or Stokes-Darcy problems and require careful formulation of the discrete problem to maintain both stability and accuracy.

This work presents a novel equal-order virtual element method for the coupled Stokes-Poisson-Boltzmann equations with several distinguishing features. We develop $\mathbb{P}_k/\mathbb{P}_k/\mathbb{P}_k$ ($k \geq 1$) virtual element approximations for velocity, pressure, and potential fields, avoiding the implementation complexity of mixed finite element spaces while maintaining theoretical rigor. To the best of our knowledge, this is the first equal-order approximation for the SPB system in both finite element and virtual element literature.

By reformulating the Laplacian drag force term $-\epsilon \Delta \psi \mathbf{E}$ using the transport potential equation, we derive a PSPG-type pressure stabilization combined with grad-div stabilization that avoids second-order derivative terms in the discrete formulation, simplifying both implementation and theoretical analysis. We establish existence and uniqueness of the weak solution using the Banach fixed-point theorem and contraction principle, while discrete well-posedness is proven via the Brouwer fixed-point theorem with explicit tracking of parameter dependencies. Optimal a priori error estimates of order $\mathcal{O}(h^k)$ are derived in the energy norm with mesh-independent constants.

The formulation naturally handles general polygonal meshes including non-convex elements and hanging nodes without special treatment, enabling adaptive refinement and irregular geometries common in nanopore sensor simulations. Comprehensive numerical experiments demonstrate optimal convergence on various mesh types (regular polygons, Voronoi tessellations, distorted meshes, meshes with hanging nodes) and validate applicability to electro-osmotic flows in nanopore sensors with T-shaped and curved obstacles at different electric field strengths.

The equal-order formulation offers several practical advantages over the mixed finite element approach of [2]: simpler implementation with uniform approximation spaces, natural handling of geometric complexity through polygonal meshes, and seamless treatment of hanging nodes for adaptive refinement. These advantages include reduced degrees of freedom (up to 43% fewer than Taylor-Hood elements for $k = 1$, and approximately 15% for $k = 2$, depending on mesh topology), simplified implementation through uniform polynomial basis handling, and high tolerance to mesh distortion. A detailed comparison with the finite element method is presented in Section 5.4.

1.1. Outline

The remaining part of the present work is sketched as follows. In Section 2, we present the coupled Stokes-Poisson-Boltzmann equations with the necessary data assumptions and the well-posedness of the primal formulation. In Section 3, we describe the pressure-stabilization method, the fundamentals of VEM, and the formulation of the stabilized virtual element discretization. In Section 5.4, we demonstrate the well-posedness of the stabilized VE problem and the error estimate in the energy norm. In Section 5, we show the practical behavior of the proposed method and its properties. In Section 6, we briefly discuss the major conclusions of the proposed work.

2. Model problem

Let Ω denote an open, bounded domain in \mathbb{R}^2 with Lipschitz boundary $\partial\Omega$, filled by an incompressible electrolyte fluid under the influence of pressure gradients and electric forces. The governing

equations involve the coupling of the Stokes and nonlinear Poisson-Boltzmann equations. The stationary case reads as: *find the velocity vector field \mathbf{u} , the scalar pressure field p , and the electrostatic double layer potential ψ satisfying:*

$$-\mu\Delta\mathbf{u} + \nabla p = \mathbf{f} - \epsilon\Delta\psi\mathbf{E} \quad \text{in } \Omega, \quad (2.1a)$$

$$\nabla \cdot \mathbf{u} = 0 \quad \text{in } \Omega, \quad (2.1b)$$

$$-\epsilon\Delta\psi + \mathbf{u} \cdot \nabla\psi + \kappa(\psi) = g \quad \text{in } \Omega, \quad (2.1c)$$

$$\mathbf{u} = \mathbf{0} \quad \text{and} \quad \psi = 0 \quad \text{on } \partial\Omega, \quad (2.1d)$$

with the additional condition that

$$\int_{\Omega} p \, d\Omega = 0, \quad (2.2)$$

where $\mu > 0$ is the fluid viscosity, \mathbf{f} a vector-valued body force, ϵ the electric permittivity of the electrolyte, \mathbf{E} an externally applied electric field (typically along the longitudinal direction), $\kappa(\psi)$ a non-linear term describing the charge of the electrolyte, and g an external load (source/sink) of potential.

Recalling [10, Lemma 2.1], we impose the following assumptions:

(A0) Data assumptions:

(i) The potential field is uniformly bounded, i.e., there exist two real constants Λ_* and Λ^* such that $\Lambda_* \leq 0 \leq \Lambda^*$ and

$$\Lambda_* \leq \psi(t) \leq \Lambda^*$$

for all $t \in \mathbb{R}$.

(ii) The nonlinear density function $\kappa(\psi)$ satisfies $\kappa(0) = 0$. Furthermore, there exist two positive constants κ_* and κ^* such that the following holds:

$$\begin{aligned} |\kappa(t_1) - \kappa(t_2)| &\leq \kappa^*|t_1 - t_2| && \text{for all } t_1, t_2 \in [\Lambda_*, \Lambda^*], \\ |\kappa(t_1) - \kappa(t_2)| &\geq \kappa_*|t_1 - t_2| && \text{for all } t_1, t_2 \in [\Lambda_*, \Lambda^*]. \end{aligned}$$

(iii) The external electric field is uniformly bounded by E^* , and also satisfies $\mathbf{E} \in [L^\infty(\Omega)]^2$.

(iv) The potential load satisfies $g \in L^2(\Omega)$.

According to (ii), we assume that $\kappa(\psi) = \alpha_0 \sinh(\alpha_1 \psi)$ where α_0 and α_1 are known positive constants. Here, α_0 depends on the ionic valence, the elementary charge, and the bulk ion concentration; α_1 is a scaling factor involving the Boltzmann constant and the reference absolute temperature.

We introduce the functional spaces for the variational formulation. For the velocity field, we define the vector-valued Sobolev space

$$\mathbf{V} := [H_0^1(\Omega)]^2 = \{\mathbf{v} \in [H^1(\Omega)]^2 : \mathbf{v} = \mathbf{0} \text{ on } \partial\Omega\},$$

equipped with the norm $\|\mathbf{v}\|_{1,\Omega} := \|\nabla\mathbf{v}\|_{\Omega}$. For the pressure field, we define the space of square-integrable functions with zero mean

$$Q := L_0^2(\Omega) = \{q \in L^2(\Omega) : \int_{\Omega} q \, d\Omega = 0\},$$

equipped with the norm $\|q\|_\Omega := \|q\|_{L^2(\Omega)}$. For the electrostatic potential, we define

$$\Phi := H^1(\Omega), \quad \Phi_0 := H_0^1(\Omega) = \{\phi \in H^1(\Omega) : \phi = 0 \text{ on } \partial\Omega\},$$

where Φ is used for the solution space and Φ_0 for the test function space, both equipped with the norm $\|\phi\|_{1,\Omega} := \|\nabla\phi\|_\Omega$ (using the Poincaré inequality for Φ_0). Additionally, we denote by V_{div} the subspace of divergence-free velocity fields

$$V_{div} := \{\mathbf{v} \in \mathbf{V} : \nabla \cdot \mathbf{v} = 0 \text{ in } \Omega\}.$$

We anticipate that we will use this last functional space in the definition of the variational form (cf. Eq. (2.8)).

2.1. Weak formulation and well-posedness

Applying the integration by parts after multiplying (2.1a)–(2.1c) by suitable test functions, we obtain the system

$$\int_\Omega \mu \nabla \mathbf{u} : \nabla \mathbf{v} d\Omega - \int_\Omega (\nabla \cdot \mathbf{v}) p d\Omega + \int_\Omega (\mathbf{u} \cdot \nabla \psi) \mathbf{E} \cdot \mathbf{v} d\Omega = \int_\Omega \mathbf{f} \cdot \mathbf{v} d\Omega + \int_\Omega (g - \kappa(\psi)) \mathbf{E} \cdot \mathbf{v} d\Omega, \quad (2.3a)$$

$$\int_\Omega (\nabla \cdot \mathbf{u}) q d\Omega = 0, \quad (2.3b)$$

$$\int_\Omega \epsilon \nabla \psi \cdot \nabla \phi d\Omega + \int_\Omega \mathbf{u} \cdot (\nabla \psi) \phi d\Omega + \int_\Omega \kappa(\psi) \phi d\Omega = \int_\Omega g \phi d\Omega, \quad (2.3c)$$

for all $(\mathbf{v}, q, \phi) \in \mathbf{V} \times Q \times \Phi_0$. We remark that Eq. (2.3a) is obtained by replacing the last drag term (Laplacian term) in the momentum equation (2.1a) by the transport potential equation (2.1c).

Given $\psi \in \Phi$ and $\mathbf{u} \in \mathbf{V}$, we introduce the bilinear forms

$$\mathcal{A}(\psi; (\mathbf{v}, q), (\mathbf{w}, r)) := a_V(\mathbf{v}, \mathbf{w}) - b(\mathbf{w}, q) + b(\mathbf{v}, r) + c(\psi; \mathbf{v}, \mathbf{w}) \quad \text{for all } (\mathbf{v}, q), (\mathbf{w}, r) \in \mathbf{V} \times Q,$$

$$\mathcal{B}(\mathbf{u}; \phi, \xi) := a_p(\phi, \xi) + c_p(\mathbf{u}; \phi, \xi) + ds(\phi, \xi) \quad \text{for all } \phi, \xi \in \Phi_0,$$

where,

$$\begin{aligned} a_V(\mathbf{v}, \mathbf{w}) &:= \int_\Omega \mu \nabla \mathbf{v} : \nabla \mathbf{w} d\Omega, & b(\mathbf{v}, q) &:= \int_\Omega (\nabla \cdot \mathbf{v}) q d\Omega, \\ c(\psi; \mathbf{v}, \mathbf{w}) &:= \int_\Omega (\mathbf{v} \cdot \nabla \psi) \mathbf{E} \cdot \mathbf{w} d\Omega, & a_p(\phi, \psi) &:= \int_\Omega \epsilon \nabla \phi \cdot \nabla \psi d\Omega, \\ c_p(\mathbf{u}; \phi, \xi) &:= \int_\Omega (\mathbf{u} \cdot \nabla \phi) \xi d\Omega, & ds(\phi, \xi) &:= \int_\Omega \kappa(\phi) \xi d\Omega. \end{aligned}$$

We note that for $\mathbf{u} \in \mathbf{V}$ such that $\nabla \cdot \mathbf{u} = 0$, the bilinear form $c_p(\mathbf{u}; \cdot, \cdot)$ satisfies the following property

$$c_p(\mathbf{u}; \phi, \xi) = -c_p(\mathbf{u}; \xi, \phi) \quad \text{for all } \phi, \xi \in \Phi_0. \quad (2.4)$$

Thus, we define the following skew-symmetric trilinear form associated with the convective term $c_p(\cdot; \cdot, \cdot)$ as follows:

$$c_p^{skew}(\mathbf{u}; \phi, \xi) = \frac{1}{2} (c_p(\mathbf{u}; \phi, \xi) - c_p(\mathbf{u}; \xi, \phi)) \quad \text{for all } \phi, \xi \in \Phi_0. \quad (2.5)$$

Finally, for given $\psi \in \Phi$, we define the load term:

$$F_\psi(\mathbf{v}) := \int_\Omega \mathbf{f} \cdot \mathbf{v} \, d\Omega + \int_\Omega (g - \kappa(\psi)) \mathbf{E} \cdot \mathbf{v} \, d\Omega \quad \text{for all } \mathbf{v} \in \mathbf{V}.$$

In view of all the above, the primal variational formulation of problem (2.1) can be stated as follows:

$$\begin{cases} \text{Find } (\mathbf{u}, p, \psi) \in \mathbf{V} \times Q \times \Phi, \text{ such that} \\ \mathcal{A}(\psi; (\mathbf{u}, p), (\mathbf{v}, q)) = F_\psi(\mathbf{v}) \quad \text{for all } (\mathbf{v}, q) \in \mathbf{V} \times Q, \\ \mathcal{B}(\mathbf{u}; \psi, \phi) = (g, \phi) \quad \text{for all } \phi \in \Phi_0. \end{cases} \quad (2.6)$$

It is obvious that the primal problem (2.6) represents a system of nonlinear equations. Therefore, problem (2.6) can be decoupled as follows:

- For any given $\psi \in \Phi$, find $(\mathbf{u}, p) \in \mathbf{V} \times Q$ such that

$$\mathcal{A}(\psi; (\mathbf{u}, p), (\mathbf{v}, q)) = F_\psi(\mathbf{v}) \quad \text{for all } (\mathbf{v}, q) \in \mathbf{V} \times Q. \quad (2.7)$$

- For any given $\mathbf{u} \in \mathbf{V}_{div}$, find $\psi \in \Phi$ such that

$$\mathcal{B}(\mathbf{u}; \psi, \phi) = (g, \phi) \quad \text{for all } \phi \in \Phi_0. \quad (2.8)$$

2.2. Well-posedness of the decoupled problems

In this section, we demonstrate the well-posedness of the decoupled problems (2.7) and (2.8).

Theorem 2.1. *Let $\psi \in \Phi$ be such that $\|\nabla\psi\|_\Omega \leq \frac{\mu}{2C_{1 \rightarrow 4}^2 E^*}$. Then, the decoupled problem (2.7) has a unique solution $(\mathbf{u}, p) \in \mathbf{V} \times Q$. Furthermore, it also satisfies*

$$\|\nabla\mathbf{u}\|_\Omega \leq \frac{2C_p}{\mu} \left(\|\mathbf{f}\|_\Omega + E^* \|g\|_\Omega + \frac{\mu\kappa^* C_p}{2C_{1 \rightarrow 4}^2} \right), \quad (2.9)$$

$$\|p\|_\Omega \leq \frac{4C_p}{\beta_0} \left(\|\mathbf{f}\|_\Omega + E^* \|g\|_\Omega + \frac{\mu\kappa^* C_p}{2C_{1 \rightarrow 4}^2} \right). \quad (2.10)$$

Proof. First, we note that the bilinear form $\mathcal{A}(\psi; \cdot, \cdot)$ is continuous. Employing the Sobolev embedding theorem and Assumption **(A0)**, for any $(\mathbf{v}, q) \in \mathbf{V} \times Q$, it holds that

$$\begin{aligned} \mathcal{A}[\psi; (\mathbf{v}, q), (\mathbf{v}, q)] &= a_V(\mathbf{v}, \mathbf{v}) + c(\psi; \mathbf{v}, \mathbf{v}) \\ &\geq \mu \|\nabla\mathbf{v}\|_\Omega^2 - E^* \|\mathbf{v}\|_{0,4,\Omega}^2 \|\nabla\psi\|_\Omega \\ &\geq (\mu - E^* C_{1 \rightarrow 4}^2 \|\nabla\psi\|_\Omega) \|\nabla\mathbf{v}\|_\Omega^2 \\ &\geq \frac{\mu}{2} \|\nabla\mathbf{v}\|_\Omega^2. \end{aligned} \quad (2.11)$$

Additionally, the bilinear form $b(\cdot, \cdot)$ satisfies the continuous inf-sup condition

$$\sup_{\mathbf{v} \in \mathbf{V} \setminus \{0\}} \frac{b(\mathbf{v}, q)}{\|\mathbf{v}\|_{1,\Omega}} \geq \beta_0 \|q\|_\Omega, \quad (2.12)$$

where $\beta_0 > 0$ is the inf-sup constant. Combining (2.11) and (2.12), the decoupled problem (2.7) has a unique solution, see [35]. Employing the Assumption **(A0)** and the Sobolev embedding theorem,

we obtain bound (2.9). Additionally, rewriting the momentum equation (2.3a) for the pressure field, we infer that

$$b(\mathbf{u}, p) = F_\psi(\mathbf{u}) - a_V(\mathbf{u}, \mathbf{u}) - c(\psi; \mathbf{u}, \mathbf{u}).$$

Recalling the discrete inf-sup condition (2.12), Assumption **(A0)**, bound (2.9), and the Sobolev embedding theorem, yield

$$\beta_0 \|p\|_\Omega \leq C_P \left(\|\mathbf{f}\|_\Omega + E^* \|g\|_\Omega + \frac{C_P \mu \kappa^*}{2C_{1 \leftrightarrow 4}^2} \right) + \frac{3\mu}{2} \|\nabla \mathbf{u}\|_\Omega.$$

Thus, we obtain inequality (2.10) from (2.9). \square

We now discuss the well-posedness of the transport potential equation (2.8) by showing that the nonlinear form $\mathcal{B}(\mathbf{u}; \cdot, \cdot)$ is strongly monotone and Lipschitz continuous.

Theorem 2.2. *For given $\mathbf{u} \in \mathbf{V}$, the problem (2.8) has a unique solution, satisfying*

$$\|\nabla \psi\|_\Omega \leq \frac{C_P}{\epsilon} \|g\|_\Omega. \quad (2.13)$$

Proof. Recalling the Lipschitz continuity of $\kappa(\cdot)$ along with the bilinear/trilinear forms $a_p(\cdot, \cdot)$ and $c_p^{skew}(\cdot, \cdot, \cdot)$, we see that $\mathcal{B}(\mathbf{u}; \cdot, \cdot)$ is Lipschitz continuous. Additionally, employing the skew-symmetric property of c_p^{skew} and Assumption **(A0)**, for any $\phi, \xi \in \Phi_0$, we find that

$$\mathcal{B}(\mathbf{u}; \phi, \phi - \xi) - \mathcal{B}(\mathbf{u}; \xi, \phi - \xi) \geq \epsilon \|\nabla(\phi - \xi)\|_\Omega^2 + \kappa_* \|\phi - \xi\|_\Omega^2 \geq \epsilon \|\nabla(\phi - \xi)\|_\Omega^2, \quad (2.14)$$

which shows that the bilinear form $\mathcal{B}(\mathbf{u}; \cdot, \cdot)$ is strongly monotone. Thus, problem (2.8) has a unique solution. \square

2.3. Well-posedness of the coupled problem

We now establish the well-posedness of the primal problem (2.6) using the Banach fixed-point theorem and the contraction principle. To achieve this goal, we reformulate problem (2.6) adopting the fixed-point strategy. Following Lemma 2.1, we introduce a well-defined operator $\mathcal{S}_{flow} : \Phi \rightarrow \mathbf{V} \times Q$, defined by

$$\mathcal{S}_{flow}(\psi) := (\mathcal{S}_{1,flow}(\psi), \mathcal{S}_{2,flow}(\psi)) =: (\mathbf{u}, p) \quad \text{for all } \psi \in \Phi, \quad (2.15)$$

where $(\mathbf{u}, p) \in \mathbf{V} \times Q$ is the unique solution of the problem (2.7) with given $\psi \in \Phi$. Recalling Lemma 2.2, we can introduce a well-defined operator $\mathcal{N}_{elec} : V_{div} \rightarrow \Phi$, defined by

$$\mathcal{N}_{elec}(\mathbf{u}) := \psi \quad \text{for all } \mathbf{u} \in \mathbf{V}_{div}, \quad (2.16)$$

where $\psi \in \Phi$ is the unique solution of (2.8) with given $\mathbf{u} \in \mathbf{V}_{div}$. Finally, we define an operator $\mathcal{T} : \Phi \rightarrow \Phi$ such that

$$\mathcal{T}(\psi) = \mathcal{N}_{elec}(\mathcal{S}_{1,flow}(\psi)) \quad \text{for all } \psi \in \Phi. \quad (2.17)$$

Thus, the fixed-point problem is stated as follows: *Find $\psi \in \Phi$, such that $\mathcal{T}(\psi) = \psi$.* We further emphasize that solving problem (2.6) is equivalent to find at least one fixed-point of \mathcal{T} . Then, we define the following closed set

$$\widehat{\Phi} := \left\{ \psi \in \Phi \text{ such that } \|\nabla \psi\|_\Omega \leq \frac{\mu}{2E^* C_{1 \leftrightarrow 4}^2} \right\}. \quad (2.18)$$

Hereafter, we first demonstrate that the operator \mathcal{T} maps $\widehat{\Phi}$ to itself.

Lemma 2.3. *Assume that the potential load $g \in L^2(\Omega)$ and the data of problem (P) satisfy the condition*

$$\frac{2C_P E^* C_{1 \leftrightarrow 4}^2}{\mu \epsilon} \|g\|_\Omega < 1. \quad (2.19)$$

Then, $\mathcal{T}(\widehat{\Phi}) \subset \widehat{\Phi}$.

Proof. Let $\psi \in \widehat{\Phi}$ such that $\mathcal{S}_{flow} = (\mathbf{u}, p)$. Recalling Lemma 2.2, we infer

$$|\mathcal{T}(\psi)|_{1,\Omega} = |\mathcal{N}_{elec}(\mathbf{u})|_{1,\Omega} \leq \frac{C_P}{\epsilon} \|g\|_\Omega \leq \frac{\mu}{2E^* C_{1 \leftrightarrow 4}^2},$$

which completes the proof. \square

Theorem 2.4. *Let $\widehat{\Phi}$ be defined by (2.18). Then, for any $\psi, \widehat{\psi} \in \widehat{\Phi}$, the operator \mathcal{T} satisfies the following*

$$|\mathcal{T}(\psi) - \mathcal{T}(\widehat{\psi})|_{1,\Omega} \leq \frac{1}{\epsilon} [\kappa^* C_P^2 + C_{1 \leftrightarrow 4}^2 |\mathcal{S}_{1,flow}(\widehat{\psi})|_{1,\Omega}] \|\nabla(\psi - \widehat{\psi})\|_\Omega. \quad (2.20)$$

Proof. Let $\psi, \widehat{\psi} \in \widehat{\Phi}$ be chosen such that

$$\mathcal{S}_{flow}(\psi) = (\mathcal{S}_{1,flow}(\psi), \text{calS}_{2,flow}(\psi)) =: (\mathbf{u}, p)$$

and

$$\mathcal{S}_{flow}(\widehat{\psi}) := (\mathcal{S}_{1,flow}(\widehat{\psi}), \mathcal{S}_{2,flow}(\widehat{\psi})) =: (\widehat{\mathbf{u}}, \widehat{p}).$$

Recalling the definition of the bilinear form $\mathcal{A}(\psi; \cdot, \cdot)$, property (2.11) and the Sobolev embedding theorem, we have

$$\begin{aligned} \frac{\mu}{2} |\mathcal{S}_{1,flow}(\psi) - \mathcal{S}_{1,flow}(\widehat{\psi})|_{1,\Omega}^2 &= \frac{\mu}{2} \|\nabla(\mathbf{u} - \widehat{\mathbf{u}})\|_\Omega^2 \\ &\leq \mathcal{A}(\psi; (\mathbf{u} - \widehat{\mathbf{u}}, p - \widehat{p}), (\mathbf{u} - \widehat{\mathbf{u}}, p - \widehat{p})) \\ &= F_\psi(\mathbf{u} - \widehat{\mathbf{u}}) - F_{\widehat{\psi}}(\mathbf{u} - \widehat{\mathbf{u}}) + \mathcal{A}(\psi - \widehat{\psi}; (\widehat{\mathbf{u}}, \widehat{p}), (\mathbf{u} - \widehat{\mathbf{u}}, p - \widehat{p})) \\ &= F_\psi(\mathbf{u} - \widehat{\mathbf{u}}) - F_{\widehat{\psi}}(\mathbf{u} - \widehat{\mathbf{u}}) + c(\psi - \widehat{\psi}; \widehat{\mathbf{u}}, \mathbf{u} - \widehat{\mathbf{u}}) \\ &\leq E^* \kappa^* \|\psi - \widehat{\psi}\|_\Omega \|\mathbf{u} - \widehat{\mathbf{u}}\|_\Omega + E^* \|\widehat{\mathbf{u}}\|_{0,4,\Omega} \|\nabla(\psi - \widehat{\psi})\|_\Omega \|\mathbf{u} - \widehat{\mathbf{u}}\|_{0,4,\Omega} \\ &\leq E^* (\kappa^* C_P^2 + C_{1 \leftrightarrow 4}^2 \|\nabla \widehat{\mathbf{u}}\|_\Omega) \|\nabla(\psi - \widehat{\psi})\|_\Omega \|\nabla(\mathbf{u} - \widehat{\mathbf{u}})\|_\Omega. \end{aligned}$$

Therefore, we get

$$|\mathcal{S}_{1,flow}(\psi) - \mathcal{S}_{1,flow}(\widehat{\psi})|_{1,\Omega} \leq \frac{2E^*}{\mu} (\kappa^* C_P^2 + C_{1 \leftrightarrow 4}^2 |\mathcal{S}_{1,flow}(\widehat{\psi})|_{1,\Omega}) \|\nabla(\psi - \widehat{\psi})\|_\Omega. \quad (2.21)$$

Then, we assume that $\mathbf{u}, \widehat{\mathbf{u}} \in \mathbf{V}_{div}$ is such that $\mathcal{N}_{elec}(\mathbf{u}) = \psi$ and $\mathcal{N}_{elec}(\widehat{\mathbf{u}}) = \widehat{\psi}$. Applying (2.14) and the Sobolev embedding Theorem yield

$$\begin{aligned} \epsilon |\mathcal{N}_{elec}(\mathbf{u}) - \mathcal{N}_{elec}(\widehat{\mathbf{u}})|_{1,\Omega}^2 &= \epsilon \|\nabla(\psi - \widehat{\psi})\|_\Omega^2 \\ &\leq \mathcal{B}(\mathbf{u}; \psi, \psi - \widehat{\psi}) - \mathcal{B}(\mathbf{u}; \widehat{\psi}, \psi - \widehat{\psi}) \\ &= \mathcal{B}(\widehat{\mathbf{u}}; \widehat{\psi}, \psi - \widehat{\psi}) - \mathcal{B}(\mathbf{u}; \widehat{\psi}, \psi - \widehat{\psi}) \\ &= c_p^{skew}(\widehat{\mathbf{u}} - \mathbf{u}; \widehat{\psi}, \psi - \widehat{\psi}) \\ &\leq C_{1 \leftrightarrow 4}^2 \|\nabla \widehat{\psi}\|_\Omega \|\nabla(\mathbf{u} - \widehat{\mathbf{u}})\|_\Omega \|\nabla(\psi - \widehat{\psi})\|_\Omega. \end{aligned}$$

Thus, we arrive at

$$|\mathcal{N}_{elec}(\mathbf{u}) - \mathcal{N}_{elec}(\widehat{\mathbf{u}})|_{1,\Omega} \leq \frac{C_{1 \leftrightarrow 4}^2}{\epsilon} |\mathcal{N}_{elec}(\widehat{\mathbf{u}})|_{1,\Omega} \|\nabla(\mathbf{u} - \widehat{\mathbf{u}})\|_{\Omega}. \quad (2.22)$$

Finally, for any $\psi, \widehat{\psi} \in \widehat{\Phi}$, we use the definition of the operator \mathcal{T} , (2.21), and (2.22):

$$\begin{aligned} |\mathcal{T}(\psi) - \mathcal{T}(\widehat{\psi})|_{1,\Omega} &= |\mathcal{N}_{elec}(\mathcal{S}_{1,flow}(\psi)) - \mathcal{N}_{elec}(\mathcal{S}_{1,flow}(\widehat{\psi}))|_{1,\Omega} \\ &\leq \frac{C_{1 \leftrightarrow 4}^2}{\epsilon} |\mathcal{T}(\widehat{\psi})|_{1,\Omega} |\mathcal{S}_{1,flow}(\psi) - \mathcal{S}_{1,flow}(\widehat{\psi})|_{1,\Omega} \\ &\leq \frac{2E^*C_{1 \leftrightarrow 4}^2}{\epsilon\mu} |\mathcal{T}(\widehat{\psi})|_{1,\Omega} [\kappa^*C_P^2 + C_{1 \leftrightarrow 4}^2 |\mathcal{S}_{1,flow}(\widehat{\psi})|_{1,\Omega}] \|\nabla(\psi - \widehat{\psi})\|_{\Omega}. \end{aligned}$$

The result (2.20) readily follows from the above analysis. \square

We remark that the operator \mathcal{T} is a continuous map on $\widehat{\Phi}$ and $\mathcal{T}(\widehat{\Phi}) \subset \widehat{\Phi}$ (see Lemma 2.3 and Theorem 2.4). Consequently, the operator \mathcal{T} has at least one fixed point using the Banach fixed-point theorem. Furthermore, the uniqueness of the fixed-point of \mathcal{T} can be achieved using the contraction principle by introducing the necessary condition on the data of the problem 2.1. Concerning this, we present the following Proposition.

Proposition 2.5. *Under the assumption of Lemma 2.3, the operator \mathcal{T} has at least one fixed-point. Hence, the coupled problem has at least one solution $(\mathbf{u}, p, \psi) \in \mathbf{V} \times Q \times \Phi$ with $\psi \in \widehat{\Phi}$, satisfying*

$$\|\nabla \mathbf{u}\|_{\Omega} + \|p\|_{\Omega} \leq \max \left\{ \frac{2C_P}{\mu}, \frac{4C_P}{\beta_0} \right\} \left(\|\mathbf{f}\|_{\Omega} + E^* \|g\|_{\Omega} + \frac{\mu\kappa^*C_P}{2C_{1 \leftrightarrow 4}^2} \right), \quad \|\nabla \psi\|_{\Omega} \leq \frac{C_P}{\epsilon} \|g\|_{\Omega}. \quad (2.23)$$

Moreover, if the data of the problem (P) satisfies

$$\frac{1}{\epsilon} \left(\kappa^*C_P^2 + \frac{2C_P C_{1 \leftrightarrow 4}^2}{\mu} \left(\|\mathbf{f}\|_{\Omega} + E^* \|g\|_{\Omega} + \frac{\mu\kappa^*C_P}{2C_{1 \leftrightarrow 4}^2} \right) \right) < 1. \quad (2.24)$$

Then the operator \mathcal{T} has a unique fixed-point. Equivalently, the primal problem (2.6) has a unique solution.

3. Stabilized virtual element framework

In this section, we present the virtual element formulation of the problem (2.6) using the equal-order approximation incorporating the residual-based pressure stabilization techniques.

For the completeness' sake, we first present the fundamentals of VEM, such as the mesh regularity assumptions, projectors, and the local/global virtual element spaces that approximate the trial and test spaces associated with the velocity vector field, pressure field, and potential field introduced in Section 2.1.

(A1) Mesh assumption.

Let E denote a generic polygonal element with boundary ∂E , area $|E|$, and diameter h_E . The barycenter and edges of polygon E are denoted by $\mathbf{x}_E \in \mathbb{R}^2$ and e , respectively. Let \mathbf{n}_E be the outward unit normal to its boundary ∂E . We consider a sequence of decompositions of Ω into non-overlapping general polygonal elements E , denoted by $\{\Omega_h\}_{h>0}$ with maximum diameter $h := \max_{h_E \in \Omega_h} h_E$. In addition, for any element $E \in \Omega_h$, we assume that there exists a constant $\delta_0 > 0$, independent of h , such that the following holds:

- each E is star-shaped with respect to a ball \mathcal{B}_E of radius $\geq \delta_0 h_E$;
- any edge $e \in \partial E$ has a finite length $|e| \geq \delta_0 |E|$.

3.1. Pressure stabilizations

We briefly review the formulation of the residual-based pressure stabilization technique for the coupled model problem (2.1). Hereafter, we introduce the following local trilinear form $\mathcal{A}_{PSPG}^E(\cdot, \cdot, \cdot)$, defined for sufficiently smooth $(\mathbf{u}, p) \in \mathbf{V} \times Q$ and for all test function pair $(\mathbf{v}, q) \times \mathbf{V} \times Q$,

$$\begin{aligned} \mathcal{A}_{PSPG}^E(\psi; (\mathbf{u}, p), (\mathbf{v}, q)) &:= a_V^E(\mathbf{u}, \mathbf{v}) - b^E(\mathbf{v}, p) + c^E(\psi; \mathbf{u}, \mathbf{v}) + b^E(\mathbf{u}, q) \\ &\quad + \mathcal{L}_1^E(p, q) + \mathcal{L}_2^E(\psi; \mathbf{u}, q), \end{aligned} \quad (3.1)$$

where the bilinear/trilinear forms $a_V^E(\cdot, \cdot)$, $b^E(\cdot, \cdot)$, and $c^E(\cdot, \cdot)$ are the local counterpart of the continuous forms $a(\cdot, \cdot)$, $b(\cdot, \cdot)$ and $c(\cdot, \cdot)$ on $P \in \Omega_h$. Furthermore, the local bilinear forms $\mathcal{L}_1^E(\cdot, \cdot)$ and $\mathcal{L}_2^E(\psi; \cdot, \cdot)$, $\psi \in \Psi$, are defined as follows:

$$\begin{aligned} \mathcal{L}_1^E(p, q) &:= \int_E \tau_E \nabla p \cdot \nabla q \, dE, \\ \mathcal{L}_2^E(\psi; \mathbf{u}, q) &:= \int_E \tau_E (-\mu \Delta \mathbf{u} + \mathbf{u} \cdot \nabla \psi \mathbf{E}) \cdot \nabla q \, dE. \end{aligned}$$

Furthermore, the corresponding local load term $F_{PSPG}^{\psi, E}(\cdot, \cdot)$ is defined by

$$F_{PSPG}^{\psi, E}(\mathbf{v}, q) := \int_E \mathbf{f} \cdot \mathbf{v} \, dE + \int_E \tau_E \mathbf{f} \cdot \nabla q \, dE + \int_E (g - \kappa(\psi)) \mathbf{E} \cdot \mathbf{v} \, dE + \int_E \tau_E (g - \kappa(\psi)) \mathbf{E} \cdot \nabla q \, dE.$$

Now, the global form of the trilinear form $\mathcal{A}_{PSPG}^E(\cdot, \cdot, \cdot)$ and load term $F_{PSPG}^{\psi, E}(\cdot, \cdot)$ are given as follows:

$$\begin{aligned} \mathcal{A}_{PSPG}(\psi; (\mathbf{u}, p), (\mathbf{v}, q)) &:= \sum_{E \in \Omega_h} \mathcal{A}_{PSPG}^E(\psi; (\mathbf{u}, p), (\mathbf{v}, q)), \\ F_{PSPG}^{\psi}(\mathbf{v}, q) &:= \sum_{E \in \Omega_h} F_{PSPG}^{\psi, E}(\mathbf{v}, q). \end{aligned}$$

Thus, the stabilized problem read as:

$$\begin{cases} \text{Find } (\mathbf{u}, p, \psi) \in \mathbf{V} \times Q \times \Phi \text{ such that} \\ \mathcal{A}_{PSPG}(\psi; (\mathbf{u}, p), (\mathbf{v}, q)) = F_{PSPG}^{\psi}(\mathbf{v}, q) & \text{for all } (\mathbf{v}, q) \in \mathbf{V} \times Q, \\ \mathcal{B}(\mathbf{u}; \psi, \phi) = (g, \phi) & \text{for all } \phi \in \Phi_0. \end{cases} \quad (3.2)$$

Remark 3.1. We remark that the stabilization of the momentum equation is considered in this work. The stabilization of the transport potential equation is not necessary for the diffusion-dominated regimes. We emphasize that the residual-based pressure stabilization technique is obtained by replacing the Laplacian term in the right-hand side of the momentum equation with the transport potential equation to avoid the higher-order derivative of the potential field. It provides a more convenient form of the stabilized problem and simplifies the implementation methodology as well as the theoretical analysis.

3.2. Projectors and virtual element spaces

In general, let E be any polygon in \mathbb{R}^2 . For $k \in \mathbb{N} \cup \{0\}$, we introduce the following definitions/notations:

- The set of monomials $\mathcal{M}_k(E)$ of degree $\leq k$:

$$\mathcal{M}_k(E) := \left\{ m_\beta \mid m_\beta = \left(\frac{\mathbf{x} - \mathbf{x}_E}{h_E} \right)^\beta \text{ with } \beta \in \mathbb{N}^2 \text{ such that } |\beta| \leq k \right\}, \quad (3.3)$$

where $\beta = (\beta_1, \beta_2)$, such that $\mathbf{x}^\beta := x_1^{\beta_1} x_2^{\beta_2}$ with $|\beta| := \beta_1 + \beta_2$.

- $\mathcal{M}_k^*(E)$: Restriction of the monomials $\mathcal{M}_k(E)$ of degree equal to k , defined by

$$\mathcal{M}_k^*(E) := \left\{ m_\beta \mid m_\beta = \left(\frac{\mathbf{x} - \mathbf{x}_E}{h_E} \right)^\beta, \beta \in \mathbb{N}^2 \text{ such that } |\beta| = k \right\}. \quad (3.4)$$

- $\mathbb{P}_k(E)$: Polynomial space of degree $\leq k$ on E , and $\mathbb{P}_{-1} = \{0\}$.
- The broken Sobolev and polynomial spaces:

$$\begin{aligned} W_p^s(\Omega_h) &:= \left\{ v \in L^2(\Omega) \text{ such that } v|_E \in W_p^s(E) \text{ for all } E \in \Omega_h \right\} \quad s \in \mathbb{R}^+, \\ \mathbb{P}_k(\Omega_h) &:= \left\{ p \in L^2(\Omega) \text{ such that } p|_E \in \mathbb{P}_k(E) \text{ for all } E \in \Omega_h \right\}. \end{aligned}$$

We recall that $W_p^s(E)$ denotes the Sobolev-Slobodeckij space of functions on E with smoothness index $s \in \mathbb{R}^+$ and integrability exponent $p \in [1, \infty]$, which coincides with the standard Sobolev space $H^k(E)$ when $s = k$ is a non-negative integer and $p = 2$.

Let us assume $E \in \Omega_h$, the following polynomial projection operators are introduced below:

- The **H¹-energy projection** operator $\Pi_k^{\nabla, E} : H^1(E) \rightarrow \mathbb{P}_k(E)$ is defined as follows:

$$\begin{cases} \int_E \nabla(\phi - \Pi_k^{\nabla, E}\phi) \cdot \nabla m_k \, dE = 0 & \text{for all } \phi \in H^1(E) \text{ and } m_k \in \mathbb{P}_k(E), \\ \int_{\partial E} (\phi - \Pi_k^{\nabla, E}\phi) \, ds = 0. \end{cases} \quad (3.5)$$

Furthermore, its extension to vector-valued function is defined by $\boldsymbol{\Pi}_k^{\nabla, E} : [H^1(E)]^2 \rightarrow [\mathbb{P}_k(E)]^2$ such that

$$\begin{cases} \int_E \nabla(\boldsymbol{\phi} - \boldsymbol{\Pi}_k^{\nabla, E}\boldsymbol{\phi}) : \nabla \mathbf{m}_k \, dE = 0 & \text{for all } \boldsymbol{\phi} \in [H^1(E)]^2 \text{ and } \mathbf{m}_k \in [\mathbb{P}_k(E)]^2, \\ \int_{\partial E} (\boldsymbol{\phi} - \boldsymbol{\Pi}_k^{\nabla, E}\boldsymbol{\phi}) \, ds = \mathbf{0}. \end{cases} \quad (3.6)$$

- The **L²-projection** operator $\Pi_k^{0, E} : L^2(E) \rightarrow \mathbb{P}_k(E)$ is given by

$$\int_E (\phi - \Pi_k^{0, E}\phi) m_k \, dE = 0 \quad \text{for all } \phi \in L^2(E) \text{ and } m_k \in \mathbb{P}_k(E). \quad (3.7)$$

Furthermore, its extension to vector-valued function is defined by $\boldsymbol{\Pi}_k^{0, E} : [L^2(E)]^2 \rightarrow [\mathbb{P}_k(E)]^2$ such that

$$\int_E (\boldsymbol{\phi} - \boldsymbol{\Pi}_k^{0, E}\boldsymbol{\phi}) \cdot \mathbf{m}_k \, dE = 0 \quad \text{for all } \boldsymbol{\phi} \in [L^2(E)]^2 \text{ and } \mathbf{m}_k \in [\mathbb{P}_k(E)]^2. \quad (3.8)$$

Remark 3.2. Stability of $\Pi_k^{0,E}$ ([34]): The L^2 -projection operator satisfies the following stability property w.r.t. L^q -norm

$$\|\Pi_k^{0,E}\phi\|_{L^q(E)} \leq C\|\phi\|_{L^q(E)} \quad \text{for all } \phi \in H^1(\Omega) \text{ and } q \geq 2. \quad (3.9)$$

We are now in a position to introduce the H^1 -conforming virtual element space $V_k^h(E)$ of order $k \in \mathbb{N}$. Following [36, 37], we introduce

$$V_k^h(E) := \left\{ \phi \in H^1(E) \text{ such that } \begin{aligned} &(i) \phi|_{\partial E} \in C^0(\partial E), \\ &(ii) \Delta\phi \in \mathbb{P}_k(E), \\ &(iii) \phi|_e \in \mathbb{P}_k(e) \quad \forall e \in \partial E, \\ &(iv) (\phi - \Pi_k^{\nabla,E}\phi, m_\alpha)_E = 0, \quad \forall m_\alpha \in \mathcal{M}_{k-1}^*(E) \cup \mathcal{M}_k^*(E) \end{aligned} \right\}.$$

Additionally, the local virtual element space is equipped with the following degrees of freedom: **DF1**(ϕ), **DF2**(ϕ), and **DF3**(ϕ):

- **DF1**(ϕ) : the values of ϕ evaluated at each vertices of E ;
- **DF2**(ϕ) : the values of ϕ evaluated at $(k-1)$ internal Gauss-Lobatto quadrature nodes on each edge $e \in \partial E$;
- **DF3**(ϕ) : the internal moments of ϕ up to order $k-2$,

$$\frac{1}{|E|} \int_E \phi m_\alpha \, dE \quad \text{for all } m_\alpha \in \mathcal{M}_{k-2}(E).$$

Finally, combining the local virtual space $V_h(E)$ for all $E \in \Omega_h$, the global virtual element space V_h is presented as follows:

$$V_h := \left\{ \phi \in H^1(\Omega) \text{ such that } \phi|_E \in V_k^h(E) \text{ for all } E \in \Omega_h \right\}.$$

After this, we define the virtual element approximations of the functional spaces introduced for the velocity vector field and pressure field, as follows:

$$\begin{aligned} \mathbf{V}^h &:= \left\{ \phi \in \mathbf{V} \text{ such that } \phi|_E \in [V_k^h(E)]^2 \text{ for all } E \in \Omega_h \right\}, \\ Q^h &:= \left\{ q \in Q \text{ such that } q|_E \in V_k^h(E) \text{ for all } E \in \Omega_h \right\}. \end{aligned}$$

Additionally, the virtual element approximation of the test and trial spaces for the potential field is defined as follows:

$$\begin{aligned} \Phi_{0,h} &:= \left\{ \phi \in \Phi_0 \text{ such that } \phi|_E \in V_k^h(E) \text{ for all } E \in \Omega_h \right\}, \\ \Phi_h &:= \left\{ \phi \in \Phi \text{ such that } \phi|_E \in V_k^h(E) \text{ for all } E \in \Omega_h \right\}. \end{aligned}$$

3.3. Discrete forms and stabilized virtual element problem

In this section, we introduce the virtual element approximation of the stabilized problem (3.2), which is computable using the **DF** degrees of freedom. We begin by introducing the discrete counterparts of the bilinear/trilinear forms and load terms.

- For any $\phi_h \in \Phi_h$, $\mathbf{v}_h, \mathbf{w}_h \in \mathbf{V}^h$, and $q_h \in Q^h$, we introduce the following local discrete counterparts associated to the first equation of (3.2):

$$\begin{aligned}
a_{V,h}^E(\mathbf{v}_h, \mathbf{w}_h) &:= \int_E \mu \boldsymbol{\Pi}_{k-1}^{0,E} \nabla \mathbf{v}_h : \boldsymbol{\Pi}_{k-1}^{0,E} \nabla \mathbf{w}_h \, dE + \mu S_1^E(\mathbf{v}_h - \boldsymbol{\Pi}_k^{\nabla,E} \mathbf{v}_h, \mathbf{w}_h - \boldsymbol{\Pi}_k^{\nabla,E} \mathbf{w}_h), \\
b_h^E(\mathbf{v}_h, q_h) &:= \int_E (\boldsymbol{\Pi}_{k-1}^{0,E} \nabla \cdot \mathbf{v}_h) \boldsymbol{\Pi}_k^{0,E} q_h \, dE, \\
c_{h,c}^E(\phi_h; \mathbf{v}_h, \mathbf{w}_h) &:= \int_E (\boldsymbol{\Pi}_k^{0,E} \mathbf{v}_h \cdot \boldsymbol{\Pi}_k^{0,E} \nabla \phi_h) \mathbf{E} \cdot \boldsymbol{\Pi}_k^{0,E} \mathbf{w}_h \, dE, \\
\mathcal{L}_{1,h}^E(p_h, q_h) &:= \int_E \tau_E \boldsymbol{\Pi}_k^{0,E} \nabla p_h \cdot \boldsymbol{\Pi}_k^{0,E} \nabla q_h \, dE + \tau_E S_2^E(p_h - \boldsymbol{\Pi}_{k-1}^{\nabla,E} p_h, q_h - \boldsymbol{\Pi}_k^{\nabla,E} q_h), \\
\mathcal{L}_{2,h}^E(\phi_h, \mathbf{u}_h, q_h) &:= \int_E \tau_E (-\nabla \cdot \boldsymbol{\Pi}_{k-1}^{0,E} \nabla \mathbf{u}_h + (\boldsymbol{\Pi}_k^{0,E} \mathbf{u}_h \cdot \boldsymbol{\Pi}_{k-1}^{0,E} \nabla \phi_h) \mathbf{E}) \cdot \boldsymbol{\Pi}_{k-1}^{0,E} \nabla q_h \, dE,
\end{aligned}$$

where $S_1^E(\cdot, \cdot) : \mathbf{V}^h(E) \times \mathbf{V}^h(E) \rightarrow \mathbb{R}$ and $S_2^E(\cdot, \cdot) : Q^h(E) \times Q^h(E) \rightarrow \mathbb{R}$ are the VEM computable symmetric positive definite bilinear forms such that they satisfy

$$\lambda_{1*} \|\nabla \mathbf{w}_h\|_{0,E}^2 \leq S_1^E(\mathbf{w}_h, \mathbf{w}_h) \leq \lambda_1^* \|\nabla \mathbf{w}_h\|_{0,E}^2 \quad \text{for all } \mathbf{w}_h \in \mathbf{V}^h(E) \cap \ker(\boldsymbol{\Pi}_k^{\nabla,E}), \quad (3.10)$$

$$\lambda_{2*} \|\nabla q_h\|_{0,E}^2 \leq S_2^E(q_h, q_h) \leq \lambda_2^* \|\nabla q_h\|_{0,E}^2 \quad \text{for all } q_h \in Q^h(E) \cap \ker(\boldsymbol{\Pi}_{k-1}^{\nabla,E}), \quad (3.11)$$

with the positive constants $\lambda_{1*} \leq \lambda_1^*$ and $\lambda_{2*} \leq \lambda_2^*$ are independent of the mesh size. Additionally, we introduce the grad-div stabilization terms to address the violation of divergence-free constraints, as follows

$$\mathcal{L}_{3,h}^E(\mathbf{v}_h, \mathbf{w}_h) := \int_E \delta_E \left(\boldsymbol{\Pi}_{k-1}^{\nabla,E} \nabla \cdot \mathbf{v}_h \right) \left(\boldsymbol{\Pi}_{k-1}^{\nabla,E} \nabla \cdot \mathbf{w}_h \right) \, dE + \delta_E S_1^E(\mathbf{v}_h - \boldsymbol{\Pi}_k^{\nabla,E} \mathbf{v}_h, \mathbf{w}_h - \boldsymbol{\Pi}_k^{\nabla,E} \mathbf{w}_h),$$

where $\delta_E > 0$ is a stabilization parameter depending on the mesh size.

Therefore, the local VEM stabilized bilinear form $\mathcal{A}_{\text{PSPG},h}^E(\phi_h; \cdot, \cdot)$ is defined by

$$\begin{aligned}
\mathcal{A}_{\text{PSPG},h}^E(\phi_h; (\mathbf{u}_h, p_h), (\mathbf{v}_h, q_h)) &:= a_{V,h}^E(\mathbf{u}_h, \mathbf{v}_h) - b_h^E(\mathbf{v}_h, p_h) + c_h^E(\phi_h; \mathbf{u}_h, \mathbf{v}_h) + b_h^E(\mathbf{u}_h, q_h) \\
&\quad + \mathcal{L}_{1,h}^E(p_h, q_h) + \mathcal{L}_{2,h}^E(\phi_h; \mathbf{u}_h, q_h) + \mathcal{L}_{3,h}^E(\mathbf{u}_h, \mathbf{v}_h), \quad (3.12)
\end{aligned}$$

for all $\phi_h \in \Phi_h(E)$, and $(\mathbf{u}_h, p_h), (\mathbf{v}_h, q_h) \in \mathbf{V}^h(E) \times Q^h(E)$. Consequently, the global trilinear form $\mathcal{A}_{\text{PSPG},h}(\phi_h; \cdot, \cdot)$ can be introduced by combining the local contributions for all $E \in \Omega_h$, as follows

$$\mathcal{A}_{\text{PSPG},h}(\phi_h; (\mathbf{u}_h, p_h), (\mathbf{v}_h, q_h)) := \sum_{E \in \Omega_h} \mathcal{A}_{\text{PSPG},h}^E(\phi_h; (\mathbf{u}_h, p_h), (\mathbf{v}_h, q_h)),$$

for all $\phi_h \in \Phi_h$, and $(\mathbf{u}_h, p_h), (\mathbf{v}_h, q_h) \in Vvh \times Q^h$. We now define the local virtual element approximation of the load term $F_{\text{PSPG}}^E(\cdot)$. For given $\phi_h \in \Phi_h(E)$, the local approximation $F_{\text{PSPG},h}^{\phi_h, E}(\cdot)$ is defined by

$$\begin{aligned}
F_{\text{PSPG},h}^{\phi_h, E}(\mathbf{v}_h, q_h) &:= \int_E \boldsymbol{\Pi}_k^{0,E} \mathbf{f} \cdot \boldsymbol{\Pi}_k^{0,E} \mathbf{v}_h \, dE + \int_E \tau_E \boldsymbol{\Pi}_k^{0,E} \mathbf{f} \cdot \boldsymbol{\Pi}_{k-1}^{0,E} \nabla q_h \, dE + \int_E (g - \kappa(\boldsymbol{\Pi}_k^{0,E} \phi_h)) \mathbf{E} \cdot \boldsymbol{\Pi}_k^{0,E} \mathbf{v}_h \, dE \\
&\quad + \int_E \tau_E (g - \kappa(\boldsymbol{\Pi}_k^{0,E} \phi_h)) \mathbf{E} \cdot \boldsymbol{\Pi}_{k-1}^{0,E} \nabla q_h \, dE.
\end{aligned}$$

Therefore, the global discrete load term is given by

$$F_{\text{PSPG},h}^{\phi_h}(\mathbf{v}_h, q_h) := \sum_{E \in \Omega_h} F_{\text{PSPG},h}^{\phi_h, E}(\mathbf{v}_h, q_h) \quad \text{for all } (\mathbf{v}_h, q_h) \in \mathbf{V}^h \times Q^h.$$

- The local discrete bilinear/trilinear form corresponding to the potential transport equation is given as follows: for any $\mathbf{v}_h \in \mathbf{V}^h(E)$ and $\phi_h, \xi_h \in \Phi_{0,h}(E)$

$$a_{p,h}^E(\phi_h, \xi_h) := \int_E \epsilon \mathbf{\Pi}_{k-1}^{0,E} \nabla \phi_h \cdot \mathbf{\Pi}_{k-1}^{0,E} \nabla \xi_h \, dE + \epsilon S_3^E(\phi_h - \Pi_k^{\nabla,E} \phi_h, \xi_h - \Pi_k^{\nabla,E} \xi_h),$$

$$c_{p,h}^E(\mathbf{v}_h; \phi_h, \xi_h) := \int_E (\mathbf{\Pi}_k^{0,E} \mathbf{v}_h \cdot \mathbf{\Pi}_{k-1}^{0,E} \nabla \phi_h) \Pi_k^{0,E} \xi_h \, dE,$$

$$c_{p,h}^{skew,E}(\mathbf{v}_h; \phi_h, \xi_h) := \frac{1}{2} (c_{p,h}^E(\mathbf{v}_h; \phi_h, \xi_h) - c_{p,h}^E(\mathbf{v}_h; \xi_h \phi_h)),$$

$$ds_h^E(\phi_h, \xi_h) := \int_E \kappa(\Pi_k^{0,E} \phi_h) \Pi_k^{0,E} \xi_h \, dE,$$

where $S_3^E(\cdot, \cdot) : \Phi_{0,h}(E) \times \Phi_{0,h}(E) \rightarrow \mathbb{R}$ is a symmetric positive definite bilinear form that satisfies

$$\lambda_{3*} \|\nabla \phi_h\|_{0,E}^2 \leq S_3^E(\phi_h, \phi_h) \leq \lambda_3^* \|\nabla \phi_h\|_{0,E}^2 \quad \text{for all } \phi_h \in \Phi_{0,h}(E) \cap \ker(\mathbf{\Pi}_k^{\nabla,E}), \quad (3.13)$$

with the positive constants $\lambda_{3*} \leq \lambda_3^*$ does not rely on the mesh size.

The discrete global form corresponding to $\mathcal{B}(\cdot, \cdot, \cdot)$ is given by

$$\mathcal{B}_h(\mathbf{v}_h; \phi_h, \xi_h) := \sum_{E \in \Omega_h} \mathcal{B}_h^E(\mathbf{v}_h; \phi_h, \xi_h),$$

where $\mathcal{B}_h^E(\mathbf{v}_h; \phi_h, \xi_h) := a_{p,h}^E(\phi_h, \xi_h) + c_{p,h}^{skew,E}(\mathbf{v}_h; \phi_h, \xi_h) + ds_h^E(\phi_h, \xi_h)$. Additionally, the discrete potential load is given by

$$(g_h, \xi_h) := \sum_{E \in \Omega_h} \int_E g \Pi_k^{0,E} \xi_h \, dE \quad \text{for all } \xi \in \Phi_{0,h}.$$

- Combining all the above, the stabilized virtual element problem is stated as follows:

$$\begin{cases} \text{Find } (\mathbf{u}_h, p_h, \psi_h) \in \mathbf{V}^h \times Q^h \times \Phi_h \text{ such that} \\ \mathcal{A}_{\text{PSPG},h}(\psi_h; (\mathbf{u}_h, p_h), (\mathbf{v}_h, q_h)) = F_{\text{PSPG},h}^{\psi_h}(\mathbf{v}_h, q_h) \quad \text{for all } (\mathbf{v}_h, q_h) \in \mathbf{V}^h \times Q^h, \\ \mathcal{B}_h(\mathbf{u}_h; \psi_h, \phi_h) = (g_h, \phi_h) \quad \text{for all } \phi_h \in \Phi_{0,h}. \end{cases} \quad (3.14)$$

Obviously, the discrete problem (3.14) can be decoupled as follows:

- With given $\psi_h \in \Phi_h$, find $(\mathbf{u}_h, p_h) \in \mathbf{V}^h \times Q^h$, such that it satisfies

$$\mathcal{A}_{\text{PSPG},h}[\psi_h; (\mathbf{u}_h, p_h), (\mathbf{v}_h, q_h)] = F_{\text{PSPG},h}^{\psi_h}(\mathbf{v}_h, q_h) \quad \text{for all } (\mathbf{v}_h, q_h) \in \mathbf{V}^h \times Q^h, \quad (3.15)$$

- With given $\mathbf{u}_h \in \mathbf{V}^h$, find $\psi_h \in \Phi_h$, such that

$$\mathcal{B}_h(\mathbf{u}_h; \psi_h, \phi_h) = (g_h, \phi_h) \quad \text{for all } \phi_h \in \Phi_{0,h}. \quad (3.16)$$

4. Theoretical analysis

We begin the theoretical analysis by first establishing the well-posedness of the discrete decoupled and coupled problems, together with a priori error estimates in the energy norm. To this end, we need to introduce some fundamental properties of Sobolev spaces. Let C_P be the Poincaré constant. Additionally, we introduce the constant $C_q > 0$, depending on Ω , such that

$$\|\phi\|_{1,\Omega} \leq C_q \|\nabla \phi\|_{\Omega} \quad \text{for all } \phi \in W_2^1(\Omega),$$

where $W_p^k(\Omega)$ denotes the Sobolev space, which reduces to $H^k(\Omega)$ when $p = 2$. Furthermore, we introduce the compact embedding constant $C_{1 \leftrightarrow p}$, corresponding to the compact embedding $H^1(\Omega) \hookrightarrow L^p(\Omega)$ for $p \geq 1$, satisfying

$$\|\phi\|_{0,p,\Omega} \leq C_{1 \leftrightarrow p} \|\nabla \phi\|_{\Omega} \quad \text{for all } \phi \in H^1(\Omega).$$

Next, we consider the fundamental inequalities and approximation estimates of Lemmas 4.1, 4.2, 4.3, and 4.4, which hold under the mesh regularity assumption **(A1)**.

Lemma 4.1 (Polynomial approximation [38]). *Under the assumption **(A1)**, for any functions $\phi \in H^s(E)$ with $E \in \Omega_h$, the elliptic projector $\Pi_k^{\nabla,E}$ and the L^2 -orthogonal projector $\Pi_k^{0,E}$ satisfy the following error estimates*

$$\|\phi - \Pi_k^{\nabla,E} \phi\|_{l,E} \leq Ch_E^{s-l} |\phi|_{s,E} \quad s, l \in \mathbb{N}, \quad s \geq 1, \quad l \leq s \leq k+1, \quad (4.1)$$

$$\|\phi - \Pi_k^{0,E} \phi\|_{l,E} \leq Ch_E^{s-l} |\phi|_{s,E} \quad s, l \in \mathbb{N}, \quad l \leq s \leq k+1. \quad (4.2)$$

Lemma 4.2 (Interpolant approximation [39]). *Under the assumption **(A1)**, for any $\phi \in H^{s+1}(E)$ there exists $\phi_I \in V_{(}^h E)$ for all $E \in \Omega_h$ such that there holds the following*

$$\|\phi - \phi_I\|_{0,E} + h_E |\phi - \phi_I|_{1,E} \leq C_{clem} h_E^{1+s} \|\phi\|_{s+1,E}, \quad 0 \leq s \leq k, \quad (4.3)$$

where the constant $C_{clem} > 0$ depends only on k and δ_0 .

Lemma 4.3 (Inverse inequality [40]). *Under the assumption **(A1)**, for any virtual element function $\phi_h \in V_{(}^h E)$ defined on $E \in \Omega_h$, it holds that*

$$|\phi_h|_{1,E} \leq C_{inv} h_E^{-1} \|\phi_h\|_{0,E}, \quad (4.4)$$

where the positive constant C_{inv} is independent of the mesh size.

Additionally, following [22, cf. Eq. (96)], we have

$$\|\Pi_{k-1}^{0,E} \nabla \mathbf{v}_h\|_{0,4,E} \leq C_{inv} h_E^{-1} \|\mathbf{v}_h\|_{0,4,E} \quad \text{for all } \mathbf{v}_h \in \mathbf{V}^h(E). \quad (4.5)$$

We now define the mesh-dependent energy norms over $\mathbf{V}^h \times Q^h$ as follows:

$$\|(\mathbf{v}_h, q_h)\|^2 = \|\nabla \mathbf{v}_h\|_{0,\Omega}^2 + \theta \|q_h\|_{0,\Omega}^2 + \mathcal{L}_{1,h}(q_h, q_h) + \mathcal{L}_{3,h}(\mathbf{v}_h, \mathbf{v}_h), \quad \text{for all } (\mathbf{v}_h, q_h) \in \mathbf{V}^h \times Q^h,$$

where the positive constant θ does not rely on the mesh size, given by

$$\theta = \frac{2\beta_0}{(3\mu\alpha^* + \alpha^* + 3\lambda_2^*) \widehat{C}_{clem}}.$$

Concerning the discrete spaces ϕ_h and $\Phi_{0,h}$, we utilize the usual H^1 -semi norm for the subsequent analysis. The stability properties of the bilinear forms $a_{V,h}(\cdot, \cdot)$ and $a_{p,h}(\cdot, \cdot)$ is discussed in the following Lemma:

Lemma 4.4. For all $\mathbf{v}_h, \mathbf{w}_h \in \mathbf{V}^h$ and $\phi_h, \xi_h \in \phi_h$, there holds the following:

$$|a_{V,h}(\mathbf{v}_h, \mathbf{w}_h)| \leq \alpha^* \mu \|\nabla \mathbf{v}_h\|_\Omega \|\nabla \mathbf{w}_h\|_\Omega, \quad (4.6)$$

$$|a_{V,h}(\mathbf{v}_h, \mathbf{v}_h)| \geq \alpha_* \mu \|\nabla \mathbf{v}_h\|_\Omega^2, \quad (4.7)$$

$$|a_{p,h}(\phi_h, \xi_h)| \leq \gamma^* \epsilon \|\nabla \phi_h\|_\Omega \|\nabla \xi_h\|_\Omega, \quad (4.8)$$

$$|a_{p,h}(\xi_h, \xi_h)| \geq \gamma_* \epsilon \|\nabla \xi_h\|_\Omega^2, \quad (4.9)$$

where $\alpha^* := \max\{1, \lambda_1^*\}$, $\alpha_* := \min\{1, \lambda_{1*}\}$, and $\gamma^* := \max\{1, \lambda_3^*\}$, $\gamma_* := \min\{1, \lambda_{3*}\}$.

Proof. The proof of Lemma 4.4 follows from [41, Lemma 5.3] with slight modification. Therefore, we skip the proof. \square

4.1. Stability of discrete decoupled problems

We now present the well-posedness of the discrete decoupled problem (3.15) by establishing the generalized discrete inf-sup condition for the velocity and pressure fields and the continuity of the bilinear form $\mathcal{A}_{\text{PSPG},h}(\psi; \cdot, \cdot)$ with given $\psi_h \in \phi_h$. Concerning this, we present the following:

Theorem 4.5. Let $\psi_h \in \phi_h$ and the stabilization parameters τ_E and δ_E satisfy the following assumptions:

$$\|\nabla \psi_h\|_\Omega \leq \frac{\alpha_* \mu}{2E^* C_{1 \leftarrow 4}^2}, \quad (4.10)$$

$$\frac{h_E^2}{\lambda_2^{*2}} \leq \tau_E \leq \frac{1}{16} \min \left\{ \frac{\alpha_*^2 h_E^2}{C_{\text{inv}}^2}; \frac{h_E^2}{C_{\text{inv}}^2} \right\} \quad \text{and} \quad \max_{E \in \Omega_h} \delta_E \leq 1 \quad \text{for all } E \in \Omega_h. \quad (4.11)$$

Also, let the physical and stabilization parameters satisfy $\mu \alpha_* \leq 2$ for small enough values of α_* . Then, for any $(\mathbf{u}_h, p_h) \in \mathbf{V}^h \times Q^h$, there exists at least one $(\mathbf{v}_h, q_h) \in \mathbf{V}^h \times Q^h$ such that the following holds

$$\sup_{(\mathbf{0}, 0) \neq (\mathbf{v}_h, q_h) \in \mathbf{V}^h \times Q^h} \frac{\mathcal{A}_{\text{PSPG},h}(\psi_h; (\mathbf{u}_h, p_h), (\mathbf{v}_h, q_h))}{\|(\mathbf{v}_h, q_h)\|} \geq \beta_* \|(\mathbf{u}_h, p_h)\|, \quad (4.12)$$

where the positive constant β_* does not rely on the mesh size and depends on the data of the problem 2.1. Furthermore, the problem (3.15) has a unique solution such that

$$\|(\mathbf{u}_h, p_h)\| \leq \frac{1}{\beta_*} \left(C_P + \frac{\alpha_* |\Omega|^{1/2}}{4C_{\text{inv}}} \right) \left(\|\mathbf{f}\|_\Omega + E^* \|g\|_\Omega + \frac{\alpha_* C_P \kappa^* \mu}{2C_{1 \leftarrow 4}^2} \right). \quad (4.13)$$

Proof. We first introduce the following settings:

$$\begin{aligned} \|(\mathbf{v}_h)\|_*^2 &= \|\nabla \mathbf{v}_h\|_{0,\Omega}^2 + \mathcal{L}_{1,h}(q_h, q_h) + \mathcal{L}_{3,h}(\mathbf{v}_h, \mathbf{v}_h), \quad \text{for all } (\mathbf{v}_h, q_h) \in \mathbf{V}^h \times Q^h. \\ &= \theta \|p_h\|_\Omega. \end{aligned}$$

Therefore, the proof of Theorem 4.5 follows in the following steps:

Step 1. With given $\psi_h \in \phi_h$, we proceed as follows

$$\begin{aligned} \mathcal{A}_{\text{PSPG},h}(\psi_h; (\mathbf{u}_h, p_h), (\mathbf{u}_h, p_h)) \\ &= a_{V,h}(\mathbf{u}_h, \mathbf{u}_h) + c_h(\psi_h; \mathbf{u}_h, \mathbf{u}_h) + \mathcal{L}_{1,h}(p_h, p_h) + \mathcal{L}_{2,h}(\psi_h; \mathbf{u}_h, p_h) + \mathcal{L}_{3,h}(\mathbf{u}_h, \mathbf{u}_h) \\ &\geq \mu \alpha_* \|\nabla \mathbf{u}_h\|_\Omega^2 + c_h(\psi_h; \mathbf{u}_h, \mathbf{u}_h) + \mathcal{L}_{1,h}(p_h, p_h) + \mathcal{L}_{2,h}(\psi_h; \mathbf{u}_h, p_h) + \mathcal{L}_{3,h}(\mathbf{u}_h, \mathbf{u}_h). \end{aligned} \quad (4.14)$$

Applying Remark 3.2, the Hölder inequality and the Sobolev embedding theorem, we have

$$\begin{aligned}
c_h(\psi_h; \mathbf{u}_h, \mathbf{u}_h) &\leq E^* \sum_{E \in \Omega_h} \|\boldsymbol{\Pi}_k^{0,E} \mathbf{u}_h\|_{0,4,E}^2 \|\nabla \psi_h\|_E \\
&\leq E^* C_{1 \leftrightarrow 4}^2 \|\nabla \mathbf{u}_h\|_\Omega^2 \|\nabla \psi_h\|_\Omega \\
&\leq \frac{\alpha_* \mu}{2} \|\nabla \mathbf{u}_h\|_\Omega^2 \quad (\text{using (4.10)})
\end{aligned} \tag{4.15}$$

Employing the Cauchy-Schwarz inequality and Lemma 4.3, it gives

$$\begin{aligned}
\mathcal{L}_{2,h}(\psi_h; \mathbf{u}_h, p_h) &\leq \sum_{E \in \Omega_h} \tau_E \| -\mu \nabla \cdot \boldsymbol{\Pi}_{k-1}^{0,E} \nabla \mathbf{u}_h + (\boldsymbol{\Pi}_k^{0,E} \mathbf{u}_h \cdot \boldsymbol{\Pi}_{k-1}^{0,E} \nabla \psi_h) \mathbf{E} \|_E \|\boldsymbol{\Pi}_{k-1}^{0,E} \nabla p_h\|_E \\
&\leq \sum_{E \in \Omega_h} \tau_E [\mu C_{inv} h_E^{-1} \|\nabla \mathbf{u}_h\|_E + E^* \|\boldsymbol{\Pi}_k^{0,E} \mathbf{u}_h\|_{0,4,E} \|\boldsymbol{\Pi}_{k-1}^{0,E} \nabla \psi_h\|_{0,4,E}] \|\boldsymbol{\Pi}_{k-1}^{0,E} \nabla p_h\|_E
\end{aligned}$$

We use the bound (4.5), Remark 3.2, the Sobolev embedding theorem and (4.10):

$$\begin{aligned}
\mathcal{L}_{2,h}(\psi_h; \mathbf{u}_h, p_h) &\leq \sum_{E \in \Omega_h} \tau_E^{1/2} [\mu C_{inv} h_E^{-1} \|\nabla \mathbf{u}_h\|_E + E^* C_{inv} h_E^{-1} \|\mathbf{u}_h\|_{0,4,E} \|\psi_h\|_{0,4,E}] \|\|\mathbf{u}_h\|\|_{*,E} \\
&\leq \max_{E \in \Omega_h} \frac{\tau_E^{1/2}}{h_E} [\mu C_{inv} \|\nabla \mathbf{u}_h\|_\Omega + E^* C_{inv} C_{1 \leftrightarrow 4}^2 \|\nabla \mathbf{u}_h\|_\Omega \|\nabla \psi_h\|_\Omega] \|\|\mathbf{u}_h\|\|_* \\
&\leq C_{inv} \max_{E \in \Omega_h} \frac{\tau_E^{1/2}}{h_E} \left(\mu + \frac{\alpha_* \mu}{2} \right) \|\|\mathbf{u}_h\|\|_*^2.
\end{aligned} \tag{4.16}$$

Combining (4.14), (4.15) and (4.16), we arrive at

$$\begin{aligned}
\mathcal{A}_{\text{PSPG},h}(\psi_h; (\mathbf{u}_h, p_h), (\mathbf{u}_h, p_h)) &\geq \frac{\mu \alpha_*}{2} \|\nabla \mathbf{u}_h\|_\Omega^2 + \mathcal{L}_{1,h}(p_h, p_h) + \mathcal{L}_{3,h}(\mathbf{u}_h, \mathbf{u}_h) - C_{inv} \max_{E \in \Omega_h} \frac{\tau_E^{1/2}}{h_E} \left(\mu + \frac{\alpha_* \mu}{2} \right) \|\|\mathbf{u}_h\|\|_*^2 \\
&\geq \left(\min \left\{ \frac{\mu \alpha_*}{2}, 1 \right\} - C_{inv} \max_{E \in \Omega_h} \frac{\tau_E^{1/2}}{h_E} \left(\mu + \frac{\alpha_* \mu}{2} \right) \right) \|\|\mathbf{u}_h\|\|_*^2 \\
&\geq \left(\frac{\mu \alpha_*}{2} - \frac{\mu \alpha_*}{4} - \frac{\mu \alpha_*}{8} \right) \|\|\mathbf{u}_h\|\|_*^2 \quad (\text{using (4.11)}) \\
&\geq \frac{\mu \alpha_*}{8} \|\|\mathbf{u}_h\|\|_*^2.
\end{aligned} \tag{4.17}$$

Note that in the second-to-last line, we use condition (4.30); see Remark 4.6.

Step 2. Using the continuous inf-sup condition for any $p_h \in Q^h$ there exists $\mathbf{w} \in \mathbf{V}$ such that

$$\int_{\Omega} (\nabla \cdot \mathbf{w}) p_h \, ds \Omega = \theta \|p_h\|_\Omega^2 \quad \text{and} \quad \|\nabla \mathbf{w}\|_\Omega \leq \frac{\theta}{\beta_0} \|p_h\|_\Omega. \tag{4.18}$$

Let $\mathbf{w}_I \in \mathbf{V}^h$ represents the virtual interpolant of $\mathbf{w} \in \mathbf{V}$. Applying Lemma 4.2, we obtain

$$\|\nabla \mathbf{w}_I\|_\Omega \leq \frac{\hat{C}_{\text{clem}} \theta}{\beta_0} \|p_h\|_\Omega, \tag{4.19}$$

where $\hat{C}_{\text{clem}} := 1 + C_{\text{clem}}$. Applying $(\mathbf{v}_h, q_h) = (-\mathbf{w}_I, 0)$ in the definition of $\mathcal{A}_{\text{PSPG},h}$, gives

$$\begin{aligned}
\mathcal{A}_{\text{PSPG},h}(\psi_h; (\mathbf{u}_h, p_h), (-\mathbf{w}_I, 0)) &= -a_{V,h}(\mathbf{u}_h, \mathbf{w}_I) + a_{bh}(\mathbf{w}_I, p_h) - c_h(\psi_h; \mathbf{u}_h, \mathbf{w}_I) - \mathcal{L}_{3,h}(\mathbf{u}_h, \mathbf{w}_I) \\
&=: -a_1 + a_2 - a_3 - a_4.
\end{aligned} \tag{4.20}$$

- We use Lemma 4.4 and (4.19):

$$a_1 \leq \alpha^* \mu \|\nabla \mathbf{u}_h\|_\Omega \|\nabla \mathbf{w}_I\|_\Omega \leq \frac{\mu \alpha^* \hat{C}_{\text{clem}} \theta}{\beta_0} \|\nabla \mathbf{u}_h\|_\Omega \|p_h\|_\Omega. \quad (4.21)$$

- Concerning a_2 , we proceed as follows

$$\begin{aligned} a_2 &= \sum_{E \in \Omega_h} \int_E \Pi_{k-1}^{0,E} (\nabla \cdot \mathbf{w}_I) \Pi_k^{0,E} p_h \, dE \\ &= \sum_{E \in \Omega_h} \left(\int_E \nabla \cdot \mathbf{w}_I (\Pi_{k-1}^{0,E} p_h - p_h) \, dE + \int_E \nabla \cdot (\mathbf{w}_I - \mathbf{w}) p_h \, dE + \int_E \nabla \cdot \mathbf{w} p_h \, dE \right). \end{aligned}$$

Concerning the second integral, we use integration by parts and the continuity property of \mathbf{w}_I , $\mathbf{w} \in \mathbf{V}$, and $p_h \in H^1(\Omega_h)$:

$$\begin{aligned} a_2 &= \sum_{E \in \Omega_h} \left(\int_E \nabla \cdot \mathbf{w}_I (\Pi_{k-1}^{0,E} p_h - p_h) \, dE - \int_E (\mathbf{w}_I - \mathbf{w}) \cdot \nabla p_h \, dE + \int_E \nabla \cdot \mathbf{w} p_h \, dE \right) \\ &= \sum_{E \in \Omega_h} \left(\int_E \nabla \cdot \mathbf{w}_I (\Pi_{k-1}^{0,E} p_h - p_h) \, dE + \int_E (\mathbf{w}_I - \mathbf{w}) \cdot (\nabla p_h - \Pi_{k-1}^{0,E} \nabla p_h) \, dE + \int_E (\mathbf{w}_I - \mathbf{w}) \cdot \Pi_{k-1}^{0,E} \nabla p_h \, dE \right. \\ &\quad \left. + \int_E \nabla \cdot \mathbf{w} p_h \, dE \right) \\ &=: a_{21} + a_{22} + a_{23} + a_{24}. \end{aligned} \quad (4.22)$$

Applying the bound (4.19) and Lemma 4.1, it holds

$$\begin{aligned} a_{21} &\leq \sum_{E \in \Omega_h} \|\nabla \mathbf{w}_I\|_E \|(I - \Pi_{k-1}^{0,E}) p_h\|_E = \sum_{E \in \Omega_h} \|\nabla \mathbf{w}_I\|_E \|(I - \Pi_{k-1}^{0,E}) (I - \Pi_{k-1}^{\nabla,E}) p_h\|_E \\ &\leq \sum_{E \in \Omega_h} h_E \|\nabla \mathbf{w}_I\|_E \|\nabla (I - \Pi_{k-1}^{\nabla,E}) p_h\|_E \\ &\leq \frac{\hat{C}_{\text{clem}} \theta}{\beta_0} \max_{E \in \Omega_h} \frac{h_E}{\tau_E^{1/2}} \|p_h\|_\Omega \mathcal{L}_{1,h}^{1/2}(p_h, p_h). \end{aligned} \quad (4.23)$$

We use Lemma 4.2, the property of the projectors, and (4.19):

$$\begin{aligned} a_{22} &\leq \sum_{E \in \Omega_h} \|\mathbf{w}_I - \mathbf{w}\|_E \|\nabla p_h - \Pi_{k-1}^{0,E} \nabla p_h\|_E \leq \sum_{E \in \Omega_h} h_E \|\nabla \mathbf{w}\|_E \|\nabla (I - \Pi_{k-1}^{\nabla,E}) p_h\|_E \\ &\leq \frac{\hat{C}_{\text{clem}} \theta}{\beta_0} \max_{E \in \Omega_h} \frac{h_E}{\tau_E^{1/2}} \|p_h\|_\Omega \mathcal{L}_{1,h}^{1/2}(p_h, p_h). \end{aligned} \quad (4.24)$$

Following the estimation of a_{22} , we infer

$$a_{23} \leq \frac{\hat{C}_{\text{clem}} \theta}{\beta_0} \max_{E \in \Omega_h} \frac{h_E}{\tau_E^{1/2}} \|p_h\|_\Omega \mathcal{L}_{1,h}^{1/2}(p_h, p_h). \quad (4.25)$$

Concerning a_{24} , we utilize (4.18). Combining the above bounds, we obtain

$$a_2 \geq \theta \|p_h\|_\Omega^2 - \frac{3\hat{C}_{\text{clem}} \theta}{\beta_0} \max_{E \in \Omega_h} \frac{h_E}{\tau_E^{1/2}} \|p_h\|_\Omega \mathcal{L}_{1,h}^{1/2}(p_h, p_h). \quad (4.26)$$

- Concerning a_3 , we use the Sobolev embedding theorem, (4.10) and (4.19):

$$a_3 \leq \frac{\mu \alpha^* \widehat{C}_{\text{clem}} \theta}{2\beta_0} \|\nabla \mathbf{u}_h\|_\Omega \|p_h\|_\Omega. \quad (4.27)$$

- Employing the bounds (3.10) and (4.19), it holds

$$a_4 \leq \alpha^* \max_{E \in \Omega_h} \delta_E \|\nabla \mathbf{u}_h\|_\Omega \|\nabla \mathbf{w}_I\|_\Omega \leq \frac{\alpha^* \widehat{C}_{\text{clem}} \theta}{\beta_0} \max_{E \in \Omega_h} \delta_E \|\nabla \mathbf{u}_h\|_\Omega \|p_h\|_\Omega. \quad (4.28)$$

Combining the bounds (4.21), (4.26), (4.27) and (4.28), and using the assumption (4.11), yields

$$\begin{aligned} \mathcal{A}_{\text{PSPG},h}(\psi_h; (\mathbf{u}_h, p_h), (-\mathbf{w}_I, 0)) &\geq \\ &\geq -\left(\frac{3\mu\alpha^* \widehat{C}_{\text{clem}} \theta}{2\beta_0} + \frac{\alpha^* \widehat{C}_{\text{clem}} \theta}{\beta_0}\right) \|\nabla \mathbf{u}_h\|_\Omega \|p_h\|_\Omega + \theta \|p_h\|_\Omega^2 - \frac{3\widehat{C}_{\text{clem}} \lambda_2^* \theta}{\beta_0} \|p_h\|_\Omega \mathcal{L}_{1,h}^{1/2}(p_h, p_h) \\ &\geq -\left(\frac{3\mu\alpha^* \widehat{C}_{\text{clem}}}{4\beta_0} + \frac{\alpha^* \widehat{C}_{\text{clem}}}{\beta_0}\right) \|\nabla \mathbf{u}_h\|_\Omega^2 + \left(\theta^{-1} - \frac{3\mu\alpha^* \widehat{C}_{\text{clem}}}{4\beta_0} - \frac{\alpha^* \widehat{C}_{\text{clem}}}{4\beta_0} - \frac{3\widehat{C}_{\text{clem}} \lambda_2^*}{4\beta_0}\right) Y^2 \\ &\quad - \frac{3\widehat{C}_{\text{clem}} \lambda_2^*}{\beta_0} \mathcal{L}_{1,h}(p_h, p_h) \\ &\geq -\frac{(4\alpha^* + 3\alpha^* \mu + 12\lambda_2^*) \widehat{C}_{\text{clem}}}{4\beta_0} \|\mathbf{u}_h\|_*^2 + \frac{(3\mu\alpha^* + \alpha^* + 3\lambda_2^*) \widehat{C}_{\text{clem}}}{4\beta_0} Y^2, \end{aligned}$$

where the last line is obtained using the definition of θ .

Step 3. We now choose $\Theta > 0$ be any constant, and $(\mathbf{v}_h, q_h) = (\mathbf{u}_h - \Theta \mathbf{w}_I, p_h)$. Therefore, we obtain the following

$$\begin{aligned} \mathcal{A}_{\text{PSPG},h}(\psi_h; (\mathbf{u}_h, p_h), (\mathbf{v}_h, q_h)) &= \mathcal{A}_{\text{PSPG},h}(\psi_h; (\mathbf{u}_h, p_h), (\mathbf{u}_h - \Theta \mathbf{w}_I, p_h)) \\ &\geq \left(\frac{\alpha_* \mu}{8} - \frac{\Theta \alpha^* (4 + 3\mu + 12\lambda_2^*) \widehat{C}_{\text{clem}}}{4\beta_0}\right) \|\mathbf{u}_h\|_*^2 + \frac{\Theta (3\mu\alpha^* + \alpha^* + 3\lambda_2^*) \widehat{C}_{\text{clem}}}{4\beta_0} Y^2 \\ &\geq \min\left\{\frac{\alpha_* \mu}{16}, \frac{\Theta}{2}\right\} \|\mathbf{u}_h\|_*^2, \end{aligned} \quad (4.29)$$

where last line is obtained using $\Theta = \mu\beta_0/4(4 + 3\mu + 12\lambda_2^*) \widehat{C}_{\text{clem}}$.

Step 4. Following [34, Lemma 10, cf. (87)], we can easily show that there exist a constant $\alpha_0 > 2$ independent of the mesh size such that $\|(\mathbf{v}_h, q_h)\|_*^2 \leq \alpha_0 \|(\mathbf{u}_h, p_h)\|_*^2$. Combining this with (4.29), we obtain the result (4.12) with $\beta_* = \frac{1}{\sqrt{\alpha_0}} \min\left\{\frac{\alpha_* \mu}{16}, \frac{\Theta}{2}\right\}$. Therefore, (3.15) has a unique solution. Moreover, it also satisfies

$$\begin{aligned} \beta_* \|(\mathbf{u}_h, p_h)\|_* \|(\mathbf{v}_h, q_h)\|_* &\leq C_P \left(\|\mathbf{f}\|_\Omega + E^* \|g\|_\Omega + C_P E^* \kappa^* \|\nabla \psi_h\|_\Omega \right) \|\nabla \mathbf{v}_h\|_\Omega \\ &\quad + \sum_{E \in \Omega_h} \tau_E^{1/2} \left(\|\mathbf{f}\|_E + E^* \|g\|_E + E^* \kappa^* \|\psi_h\|_E \right), \|(\mathbf{v}_h, q_h)\|_E \\ &\leq \left(C_P + \frac{|\Omega|^{1/2}}{4C_{\text{inv}}} \right) \left(\|\mathbf{f}\|_\Omega + E^* \|g\|_\Omega + C_P E^* \kappa^* \|\nabla \psi_h\|_\Omega \right) \|(\mathbf{v}_h, q_h)\|. \end{aligned}$$

Thus, the result (4.13) follows from the above analysis. \square

Remark 4.6. The coercivity estimate (4.17) in the proof of Theorem 4.5 relies on the identity $\min\left\{\frac{\mu\alpha_*}{2}, 1\right\} = \frac{\mu\alpha_*}{2}$, which holds under the condition

$$\mu\alpha_* \leq 2. \quad (4.30)$$

Since $\alpha_* = \min\{1, \lambda_1\} \leq 1$ by definition, condition (4.30) is automatically satisfied whenever $\mu \leq 2$. For the parameter regimes that we will consider in the numerical experiments of Section 6, where $\mu = 1$ (Examples 1 and 2) and $\mu = 0.1$ (Example 3), this condition holds with a comfortable margin. We note that even when $\mu > 2$, the proof can be adapted by retaining the minimum in the coercivity constant, which leads to $\min\left\{\frac{\mu\alpha_*}{2}, 1\right\}$ replacing $\frac{\mu\alpha_*}{2}$ in (4.17) and all subsequent estimates that depend on it. A thorough discussion about this topic is also reported in Section 4.4.

Hereafter, we discuss the existence and uniqueness of the discrete solution to the potential transport equation (3.16). Following the continuous case Lemma 2.2, the nonlinear form $\mathcal{B}_h(\mathbf{u}_h; \cdot, \cdot)$ satisfies the strongly monotone property (using the strongly monotone property of $\kappa(\cdot)$) and Lipschitz continuity. Here, we use the Brouwer fixed-point theorem to show the well-posedness of the problem (3.16).

Theorem 4.7. *For any fixed $\mathbf{u}_h \in \mathbf{V}^h$, the discrete problem (3.16) has a unique solution $\psi_h \in \Phi_h$, satisfying*

$$\|\nabla\psi_h\|_\Omega \leq \frac{C_P}{\epsilon\gamma_*} \|g\|_\Omega. \quad (4.31)$$

Proof. The proof of Theorem 4.7 follows from the Brouwer fixed-point theorem on the finite-dimensional spaces with some modification in the proof of [41, Theorem 5.5]. In addition, it also holds

$$\epsilon\gamma_*\|\nabla\psi_h\|_\Omega \leq \sum_{E \in \Omega_h} \|g\|_E \|\psi_h\|_E \leq C_P \|g\|_\Omega \|\nabla\psi_h\|_\Omega.$$

Thus, the stability estimate (4.31) readily follows from the above analysis. \square

4.2. Well-posedness of the stabilized virtual element problem

We are now in a position to demonstrate the well-posedness of the stabilized problem (3.14). To do this, we adopt the fixed-point approach utilized in the continuous case to reformulate the problem (3.2) into an equivalent fixed-point problem. In view of Theorem 4.5, we introduce a well-defined discrete operator $\mathcal{S}_{flow}^h : \phi_h \rightarrow \mathbf{V}^h \times Q^h$ such that

$$\psi_h \rightarrow \mathcal{S}_{flow}^h := (\mathcal{S}_{1,flow}^h(\psi_h), \mathcal{S}_{2,flow}^h(\psi_h)) =: (\mathbf{u}_h, p_h) \quad \text{for all } \psi_h \in \phi_h, \quad (4.32)$$

where $(\mathbf{u}_h, p_h) \in \mathbf{V}^h \times Q^h$ is the unique solution of (3.15) with given $\psi_h \in \phi_h$ satisfying the assumption of Theorem 4.5. Following Theorem 4.7, we introduce a well-defined map $\mathcal{N}_{elec}^h : \mathbf{V}^h \rightarrow \phi_h$ such that

$$\mathbf{u}_h \rightarrow \mathcal{N}_{elec}^h(\mathbf{u}_h) = \psi_h \quad \text{for all } \mathbf{u}_h \in \mathbf{V}^h, \quad (4.33)$$

where $\psi_h \in \phi_h$ is the unique solution of (3.16) with given $\mathbf{u}_h \in \mathbf{V}^h$. Mimicking the continuous case, we introduce an operator $\mathcal{T}^h : \phi_h \rightarrow \phi_h$ such that

$$\mathcal{T}^h(\psi_h) = \mathcal{N}^h(\mathcal{S}_{1,flow}^h(\psi_h)) \quad \text{for all } \psi_h \in \phi_h. \quad (4.34)$$

Finally, we introduce the equivalent discrete fixed-point problem as follows: *Find $\psi_h \in \phi_h$ such that $\mathcal{T}^h(\psi_h) = \psi_h$.* Therefore, seeking the fixed point of \mathcal{T}^h will be equivalent to solving the stabilized problem (3.14).

Lemma 4.8. *We define $\widehat{\Phi}_h := \{\phi_h \in \phi_h \text{ such that } \|\nabla \phi_h\|_\Omega \leq r\}$ with an arbitrary constant r . Let the data of the problem be such that*

$$\frac{C_P}{\epsilon \gamma_*} \|g\|_\Omega \leq \frac{\alpha_* \mu}{2E^* C_{1 \leftrightarrow 4}^2} \leq r. \quad (4.35)$$

Then, $\mathcal{T}^h(\widehat{\Phi}_h) \subset \widehat{\Phi}_h$.

Proof. The proof follows from Lemma 2.3. \square

Lemma 4.9. *Under the assumption of Lemma 4.8, for any $\psi_h, \widehat{\psi}_h \in \widehat{\Phi}_h$, the discrete operator \mathcal{T}^h satisfies the following*

$$\begin{aligned} |\mathcal{T}^h(\psi_h) - \mathcal{T}^h(\widehat{\psi}_h)|_{1,\Omega} &\leq \frac{rE^* C_{1 \leftrightarrow 4}^2}{\gamma_* \epsilon \beta_*} \left(C_P^2 \kappa^* + \frac{C_P \kappa^* |\Omega|^{1/2}}{4C_{inv}} + \frac{5}{4} C_{1 \leftrightarrow 4}^2 |\mathcal{S}_{1,flow}^h(\widehat{\psi})|_{1,\Omega} \right) \cdot \\ &\quad \cdot \|\nabla(\psi_h - \widehat{\psi}_h)\|_\Omega. \end{aligned} \quad (4.36)$$

Proof. The proof of Lemma 4.9 follows from the following three steps.

Step 1. We choose $\psi_h, \widehat{\psi}_h \in \widehat{\Phi}_h$ such that

- $\mathcal{S}_{flow}^h(\psi_h) = (\mathcal{S}_{1,flow}^h(\psi_h), \mathcal{S}_{2,flow}^h(\psi_h)) =: (\mathbf{u}_h, p_h)$;
- $\mathcal{S}_{flow}^h(\widehat{\psi}_h) := (\mathcal{S}_{1,flow}^h(\widehat{\psi}_h), \mathcal{S}_{2,flow}^h(\widehat{\psi}_h)) =: (\widehat{\mathbf{u}}_h, \widehat{p}_h)$.

Employing the discrete inf-sup inequality (4.12), it gives

$$\begin{aligned} \beta_* |||\mathcal{S}_{flow}^h(\psi_h) - \mathcal{S}_{flow}^h(\widehat{\psi}_h)||| |||(\mathbf{v}_h, q_h)||| &\leq \mathcal{A}_{PSPG,h}(\psi_h; (\mathbf{u}_h - \widehat{\mathbf{u}}_h, p_h - \widehat{p}_h), (\mathbf{v}_h, q_h)) \\ &= F_{PSPG,h}^{\psi_h}(\mathbf{v}_h, q_h) - F_{PSPG,h}^{\widehat{\psi}_h}(\mathbf{v}_h, q_h) + \mathcal{A}_{PSPG,h}(\widehat{\psi}_h - \psi_h; (\widehat{\mathbf{u}}_h, \widehat{p}_h), (\mathbf{v}_h, q_h)). \end{aligned} \quad (4.37)$$

Expanding the terms on the right, we obtain

$$\begin{aligned} &F_{PSPG,h}^{\psi_h}(\mathbf{v}_h, q_h) - F_{PSPG,h}^{\widehat{\psi}_h}(\mathbf{v}_h, q_h) + \mathcal{A}_{PSPG,h}(\widehat{\psi}_h - \psi_h; (\widehat{\mathbf{u}}_h, \widehat{p}_h), (\mathbf{v}_h, q_h)) \\ &= \sum_{E \in \Omega_h} \left(\int_E (\kappa(\Pi_k^{0,E} \psi_h) - \kappa(\Pi_k^{0,E} \widehat{\psi}_h)) \mathbf{E} \cdot \mathbf{\Pi}_k^{0,E} \mathbf{v}_h dE \right. \\ &\quad + \int_E \tau_E (\kappa(\Pi_k^{0,E} \psi_h) - \kappa(\Pi_k^{0,E} \widehat{\psi}_h)) \mathbf{E} \cdot \mathbf{\Pi}_{k-1}^{0,E} \nabla q_h dE \\ &\quad + \int_E \mathbf{\Pi}_k^{0,E} \mathbf{u}_h \cdot \mathbf{\Pi}_{k-1}^{0,E} \nabla(\widehat{\psi}_h - \psi_h) \mathbf{E} \cdot \mathbf{\Pi}_k^{0,E} \mathbf{v}_h dE \\ &\quad \left. + \int_E \tau_E (\mathbf{\Pi}_k^{0,E} \mathbf{u}_h \cdot \mathbf{\Pi}_{k-1}^{0,E} \nabla(\widehat{\psi}_h - \psi_h)) \mathbf{E} \cdot \mathbf{\Pi}_{k-1}^{0,E} \nabla q_h dE \right) \\ &\leq \sum_{E \in \Omega_h} \left(E^* \kappa^* \|\psi_h - \widehat{\psi}_h\|_E \|\mathbf{v}_h\|_E + E^* \kappa^* \tau_E \|\psi_h - \widehat{\psi}_h\|_E \|\mathbf{\Pi}_{k-1}^{0,E} \nabla q_h\|_E \right. \\ &\quad + E^* \|\nabla(\psi_h - \widehat{\psi}_h)\|_E \|\mathbf{u}_h\|_{0,4,E} \|\mathbf{v}_h\|_{0,4,E} \\ &\quad \left. + E^* \tau_E \|\mathbf{\Pi}_{k-1}^{0,E} \nabla(\psi_h - \widehat{\psi}_h)\|_{0,4,E} \|\mathbf{u}_h\|_{0,4,E} \|\mathbf{\Pi}_{k-1}^{0,E} \nabla q_h\|_E \right). \end{aligned} \quad (4.38)$$

Combining the estimates and using the bounds from Remark 3.2, inequality (4.5), the Sobolev embedding theorem, and $\tau_E \leq h_E^2/16C_{inv}$, we deduce

$$\begin{aligned} & \sum_{E \in \Omega_h} \left(E^* \kappa^* \|\psi_h - \hat{\psi}_h\|_E \|\mathbf{v}_h\|_E + E^* \kappa^* \tau_E \|\psi_h - \hat{\psi}_h\|_E \|\mathbf{\Pi}_{k-1}^{0,E} \nabla q_h\|_E \right. \\ & \quad \left. + E^* \|\nabla(\psi_h - \hat{\psi}_h)\|_E \|\mathbf{u}_h\|_{0,4,E} \|\mathbf{v}_h\|_{0,4,E} + E^* \tau_E \|\mathbf{\Pi}_{k-1}^{0,E} \nabla(\psi_h - \hat{\psi}_h)\|_{0,4,E} \|\mathbf{u}_h\|_{0,4,E} \|\mathbf{\Pi}_{k-1}^{0,E} \nabla q_h\|_E \right) \\ & \leq E^* \left(C_P^2 \kappa^* + \frac{C_P \kappa^* |\Omega|^{1/2}}{4C_{inv}} + (C_{1 \rightarrow 4}^2 + \frac{1}{4} C_{1 \rightarrow 4}^2) \|\nabla \hat{\mathbf{u}}_h\|_\Omega \right) \|\nabla(\psi_h - \hat{\psi}_h)\|_\Omega \|\mathbf{v}_h, q_h\|, \end{aligned} \quad (4.39)$$

Applying the definition of $\mathcal{S}_{\text{flow}}^h$, it holds

$$\|\mathcal{S}_{\text{flow}}^h(\psi_h) - \mathcal{S}_{\text{flow}}^h(\hat{\psi}_h)\| \leq \frac{E^*}{\beta_*} \left(C_P^2 \kappa^* + \frac{C_P \kappa^* |\Omega|^{1/2}}{4C_{inv}} + \frac{5}{4} C_{1 \rightarrow 4}^2 |\mathcal{S}_{1,\text{flow}}^h(\hat{\psi})|_{1,\Omega} \right), \|\nabla(\psi_h - \hat{\psi}_h)\|_\Omega. \quad (4.40)$$

Step 2. Let $\mathbf{u}_h, \hat{\mathbf{u}}_h \in \mathbf{V}^h$ such that $\mathcal{N}_{\text{elec}}^h(\mathbf{u}_h) = \psi_h$ and $\mathcal{N}_{\text{elec}}^h(\hat{\mathbf{u}}_h) = \hat{\psi}_h$. We use the stability property of $a_{p,h}$ (cf. Lemma 4.4) and the strongly monotone property of $\kappa(\cdot)$:

$$\begin{aligned} & \gamma_* \epsilon |\mathcal{N}_{\text{elec}}^h(\mathbf{u}_h) - \mathcal{N}_{\text{elec}}^h(\hat{\mathbf{u}}_h)|_{1,\Omega}^2 = \gamma_* \epsilon \|\nabla(\psi_h - \hat{\psi}_h)\|_\Omega^2 \\ & \leq \mathcal{B}_h(\mathbf{u}_h; \psi_h, \psi_h - \hat{\psi}_h) - \mathcal{B}_h(\mathbf{u}_h; \hat{\psi}_h, \psi_h - \hat{\psi}_h) = \mathcal{B}_h(\hat{\mathbf{u}}_h; \hat{\psi}_h, \psi_h - \hat{\psi}_h) - \mathcal{B}_h(\mathbf{u}_h; \hat{\psi}_h, \psi_h - \hat{\psi}_h) \\ & = c_{p,h}^{\text{skew}}(\hat{\mathbf{u}}_h - \mathbf{u}_h; \hat{\psi}_h, \psi_h - \hat{\psi}_h) \leq C_{1 \rightarrow 4}^2 \|\nabla \hat{\psi}_h\|_\Omega \|\nabla(\mathbf{u}_h - \hat{\mathbf{u}}_h)\|_\Omega \end{aligned}$$

Thus, we arrive at

$$|\mathcal{N}_{\text{elec}}^h(\mathbf{u}_h) - \mathcal{N}_{\text{elec}}^h(\hat{\mathbf{u}}_h)|_{1,\Omega} \leq \frac{C_{1 \rightarrow 4}^2}{\gamma_* \epsilon} |\mathcal{N}_{\text{elec}}^h(\hat{\mathbf{u}}_h)|_{1,\Omega} \|\nabla(\mathbf{u}_h - \hat{\mathbf{u}}_h)\|_\Omega. \quad (4.41)$$

Step 3. Recalling (4.40) and (4.41), and we proceed as follows

$$\begin{aligned} |\mathcal{T}^h(\psi_h) - \mathcal{T}^h(\hat{\psi}_h)|_{1,\Omega} &= |\mathcal{N}_{\text{elec}}^h(\mathcal{S}_{1,\text{flow}}^h(\psi_h)) - \mathcal{N}_{\text{elec}}^h(\mathcal{S}_{1,\text{flow}}^h(\hat{\psi}_h))|_{1,\Omega} \\ &\leq \frac{C_{1 \rightarrow 4}^2}{\gamma_* \epsilon} |\mathcal{T}^h(\hat{\psi}_h)|_{1,\Omega} |\mathcal{S}_{1,\text{flow}}^h(\psi_h) - \mathcal{S}_{1,\text{flow}}^h(\hat{\psi}_h)|_{1,\Omega}. \end{aligned}$$

Thus, (4.36) can be easily obtained from (4.40). \square

Following the continuous case, the discrete operator \mathcal{T}^h has at least one fixed point using the Brouwer fixed-point theorem (cf. Lemmas 4.8 and 4.9). Furthermore, the uniqueness of the fixed-point of \mathcal{T}^h can be demonstrated by introducing the necessary condition on the data of the problem (P) . We summarize the existence and uniqueness of the fixed-point problem in the following Proposition.

Proposition 4.10. *Under the assumption of Lemma 4.8, the operator \mathcal{T}^h has at least one fixed-point. Thus, the stabilized virtual element problem (3.14) has at least one solution $(\mathbf{u}_h, p_h, \psi_h) \in \mathbf{V}^h \times Q^h \times \phi_h$ with $\psi \in \hat{\Phi}_h$ such that there holds*

$$\|\mathbf{u}_h, p_h\| \leq \frac{1}{\beta_*} \left(C_P + \frac{\alpha_* |\Omega|^{1/2}}{4C_{inv}} \right) \left(\|\mathbf{f}\|_\Omega + E^* \|g\|_\Omega + \frac{\alpha_* C_P \kappa^* \mu}{2C_{1 \rightarrow 4}^2} \right), \quad \|\nabla \psi\|_\Omega \leq \frac{C_P}{\gamma_* \epsilon} \|g\|_\Omega. \quad (4.42)$$

Moreover, if the data of problem (2.1) satisfies the following:

$$\frac{rE^*C_{1 \leftarrow 4}^2}{\gamma_*\epsilon\beta_*} \left(C_P^2\kappa^* + \frac{C_P\kappa^*|\Omega|^{1/2}}{4C_{inv}} + \frac{5C_{1 \leftarrow 4}^2}{4\beta_*} \left(C_P + \frac{\alpha_*|\Omega|^{1/2}}{4C_{inv}} \right) \left(\|\mathbf{f}\|_\Omega + E^*\|g\|_\Omega + \frac{\alpha_*C_P\kappa^*\mu}{2C_{1 \leftarrow 4}^2} \right) \right) < 1. \quad (4.43)$$

Then, the operator \mathcal{T}^h has a unique fixed-point. Equivalently, the problem (3.14) has a unique solution.

4.3. A priori error estimate

In this section, we derive a priori error estimates in the energy norm with optimal convergence rates. Throughout this section, the virtual interpolant of $(\mathbf{u}, p, \psi) \in \mathbf{V} \times Q \times \Phi$ is denoted by $(\mathbf{u}_I, p_I, \psi_I) \in \mathbf{V}^h \times Q^h \times \phi_h$. We first introduce the following regularity condition to derive the error estimate:

(A2) Regularity assumptions:

$$\begin{aligned} \mathbf{u} &\in \mathbf{V} \cap [H^{k+1}(\Omega_h)]^2, & p &\in Q \cap H^k(\Omega_h), & \psi &\in \Phi \cap H^{k+1}(\Omega_h), & \mathbf{f} &\in [H^{k-1}(\Omega_h)]^2, \\ g &\in H^{k-1}(\Omega_h), & \mathbf{E} &\in [W^{k-1,\infty}(\Omega_h)]^2, & \kappa &\in H^{k-1}(\Omega_h). \end{aligned}$$

Hereafter, we use $\|\nabla \mathbf{u}\|_\cdot \leq C_u$ (cf. the bound (2.9)) in the subsequent analysis. Furthermore, the constant C is independent of the mesh size and also depends on the data of the problem (2.1), the mesh regularity constant, and the stability constants.

Lemma 4.11. *With the assumption (A2) and the hypothesis of Theorems 4.5 and 2.1, we consider $(\mathbf{u}_I, p_I) \in \mathbf{V}^h \times Q^h$ denotes the virtual interpolant of $(\mathbf{u}, p) \in \mathbf{V} \times Q$. Furthermore, for given $\psi \in \Phi$ and $\psi_h \in \Phi_h$, let $(\mathbf{u}, p) \in \mathbf{V} \times Q$ and $(\mathbf{u}_h, p_h) \in \mathbf{V}^h \times Q^h$ be the solution of problems (2.7) and (3.15), respectively. Then, for all $(\mathbf{v}_h, q_h) \in \mathbf{V}^h \times Q^h$, the following holds*

$$\begin{aligned} \mathcal{A}_{\text{PSPG}}(\psi; (\mathbf{u}, p), (\mathbf{v}_h, q_h)) - \mathcal{A}_{\text{PSPG},h}(\psi_h; (\mathbf{u}_I, p_I), (\mathbf{v}_h, q_h)) &\leq Ch^k \left(\|\mathbf{u}\|_{k+1,\Omega} + \|p\|_{k,\Omega} + \|\psi\|_{k+1,\Omega} \right. \\ &\quad \left. + \max_{E \in \Omega_h} \|\mathbf{E}\|_{k-1,\infty,E} \|\mathbf{u}\|_{k+1,\Omega} \|\psi\|_{k+1,\Omega} + \|\psi\|_{2,\Omega} \|\mathbf{u}\|_{k+1,\Omega} \right) |||(\mathbf{v}_h, q_h)||| \\ &\quad + \frac{5E^*C_{1 \leftarrow 4}^2}{4} \|\nabla \mathbf{u}\|_\Omega \|\nabla(\psi_I - \psi_h)\|_\Omega |||(\mathbf{v}_h, q_h)|||. \end{aligned} \quad (4.44)$$

Proof. Using the definition of $\mathcal{A}_{\text{PSPG}}$ and $\mathcal{A}_{\text{PSPG},h}$, we have

$$\begin{aligned} \mathcal{A}_{\text{PSPG}}(\psi; (\mathbf{u}, p), (\mathbf{v}_h, q_h)) - \mathcal{A}_{\text{PSPG},h}(\psi_h; (\mathbf{u}_I, p_I), (\mathbf{v}_h, q_h)) &= a_V(\mathbf{u}, \mathbf{v}_h) - a_{V,h}(\mathbf{u}_I, \mathbf{v}_h) + a_{bh}(\mathbf{v}_h, p_I) - a_b(\mathbf{v}_h, p) + a_b(\mathbf{u}, q_h) - a_{bh}(\mathbf{u}_I, q_h) + \\ &\quad a_c(\psi; \mathbf{u}, \mathbf{v}_h) - c_h(\psi_h; \mathbf{u}_I, \mathbf{v}_h) + \mathcal{L}_1(p, q_h) - \mathcal{L}_{1,h}(p_I, q_h) + \\ &\quad \mathcal{L}_2(\psi; \mathbf{u}, q_h) - \mathcal{L}_{2,h}(\psi_h; \mathbf{u}_I, q_h) - \mathcal{L}_{3,h}(\mathbf{u}_I, \mathbf{v}_h). \\ &=: \eta_1 + \eta_2 + \eta_3 + \eta_4 + \eta_5 + \eta_6 - \eta_7. \end{aligned} \quad (4.45)$$

The estimation of the above involves the following steps:

Step 1. Following [33, Lemma 7], we obtain the followings

$$\begin{aligned} |\eta_1 + \eta_2 + \eta_3| &\leq |a_V(\mathbf{u}, \mathbf{v}_h) - a_{V,h}(\mathbf{u}_I, \mathbf{v}_h)| + |a_{bh}(\mathbf{v}_h, p_I) - a_b(\mathbf{v}_h, p)| + |a_b(\mathbf{u}, q_h) - a_{bh}(\mathbf{u}_I, q_h)| \\ &\leq Ch^k (\|\mathbf{u}\|_{k+1,\Omega} + \|p\|_{k,\Omega}) |||(\mathbf{v}_h, q_h)|||. \end{aligned} \quad (4.46)$$

Step 2. Adding and subtracting suitable terms, we infer

$$\begin{aligned}
\eta_4 &= \sum_{E \in \Omega_h} \left(\int_E (\mathbf{u} \cdot \nabla \psi) \mathbf{E} \cdot \mathbf{v}_h dE - \int_E (\mathbf{\Pi}_k^{0,E} \mathbf{u}_I \cdot \mathbf{\Pi}_{k-1}^{0,E} \nabla \psi_h) \mathbf{E} \cdot \mathbf{\Pi}_k^{0,E} \mathbf{v}_h dE \right) \\
&= \sum_{E \in \Omega_h} \left(\int_E (\mathbf{u} \cdot \nabla \psi) \mathbf{E} \cdot (\mathbf{v}_h - \mathbf{\Pi}_k^{0,E} \mathbf{v}_h) dE + \int_E ((\mathbf{u} - \mathbf{\Pi}_k^{0,E} \mathbf{u}_I) \cdot \nabla \psi) \mathbf{E} \cdot \mathbf{\Pi}_k^{0,E} \mathbf{v}_h dE \right. \\
&\quad \left. + \int_E \mathbf{\Pi}_k^{0,E} \mathbf{u}_I \cdot (\nabla \psi - \mathbf{\Pi}_{k-1}^{0,E} \nabla \psi_I) \mathbf{E} \cdot \mathbf{\Pi}_k^{0,E} \mathbf{v}_h dE + \int_E \mathbf{\Pi}_k^{0,E} \mathbf{u}_I \cdot \mathbf{\Pi}_{k-1}^{0,E} (\nabla \psi_I - \nabla \psi_h) \mathbf{E} \cdot \mathbf{\Pi}_k^{0,E} \mathbf{v}_h dE \right) \\
&=: \eta_{41} + \eta_{42} + \eta_{43} + \eta_{44}. \tag{4.47}
\end{aligned}$$

- We recall the orthogonality property of the projection operator, Lemma 4.1, and regularity assumption **(A2)**:

$$\begin{aligned}
\eta_{41} &= \sum_{E \in \Omega_h} \int_E \left((\mathbf{u} \cdot \nabla \psi) \mathbf{E} - \mathbf{\Pi}_{k-1}^{0,E} (\mathbf{u} \cdot \nabla \psi \mathbf{E}) \right) \cdot (\mathbf{v}_h - \mathbf{\Pi}_k^{0,E} \mathbf{v}_h) dE \\
&\leq C \sum_{E \in \Omega_h} \|\mathbf{E}\|_{k-1,\infty,E} h_E^k |\mathbf{u} \cdot \nabla \psi|_{k-1,E} \|\nabla \mathbf{v}_h\|_E \\
&\leq Ch^k \max_{E \in \Omega_h} \|\mathbf{E}\|_{k-1,\infty,E} |\mathbf{u}|_{k-1,4,\Omega} \|\nabla \psi\|_{k-1,4,\Omega} \|\nabla \mathbf{v}_h\|_\Omega \\
&\leq Ch^k \max_{E \in \Omega_h} \|\mathbf{E}\|_{k-1,\infty,E} \|\mathbf{u}\|_{k+1,\Omega} \|\psi\|_{k+1,\Omega} |||(\mathbf{v}_h, q_h)|||. \tag{4.48}
\end{aligned}$$

- Concerning η_{42} , we proceed as follows

$$\begin{aligned}
\eta_{42} &\leq C \sum_{E \in \Omega_h} \|(\mathbf{u} - \mathbf{\Pi}_k^{0,E} \mathbf{u}_I)\|_E \|\nabla \psi\|_{0,4,E} \|\mathbf{v}_h\|_{0,4,E} \\
&\leq \sum_{E \in \Omega_h} h_E^{k+1} \|\mathbf{u}\|_{k+1,E} \|\nabla \psi\|_{0,4,E} \|\mathbf{v}_h\|_{0,4,E} \\
&\leq Ch^{k+1} \|\mathbf{u}\|_{k+1,\Omega} \|\psi\|_{2,\Omega} |||(\mathbf{v}_h, q_h)|||. \tag{4.49}
\end{aligned}$$

- Applying Remark 3.2, the Sobolev embedding theorem, and Lemmas 4.1 and 4.2, it gives

$$\begin{aligned}
\eta_{43} &\leq \sum_{E \in \Omega_h} \|\mathbf{u}_I\|_{0,4,E} \|\nabla \psi - \mathbf{\Pi}_{k-1}^{0,E} \nabla \psi_I\|_E \|\mathbf{v}\|_{0,4,E} \\
&\leq Ch^k \|\mathbf{u}_I\|_{0,4,\Omega} \|\psi\|_{k+1,\Omega} \|\mathbf{v}\|_{0,4,\Omega} \\
&\leq Ch^k \|\psi\|_{k+1,\Omega} |||(\mathbf{v}, q)|||. \tag{4.50}
\end{aligned}$$

- Using the stability property of L^2 -projectors, the Sobolev embedding theorem and Hölder inequality, we obtain

$$\begin{aligned}
\eta_{44} &\leq E^* \sum_{E \in \Omega_h} \|\mathbf{u}_I\|_{0,4,E} \|\nabla \psi_I - \nabla \psi_h\|_E \|\mathbf{v}_h\|_{0,4,E} \\
&\leq E^* C_{1 \leftrightarrow 4}^2 \|\nabla \mathbf{u}_I\|_\Omega \|\nabla \psi_I - \nabla \psi_h\|_\Omega \|\nabla \mathbf{v}_h\|_\Omega \\
&\leq E^* C_{1 \leftrightarrow 4}^2 \|\nabla \mathbf{u}\|_\Omega \|\nabla \psi_I - \nabla \psi_h\|_\Omega |||(\mathbf{v}_h, q_h)|||. \tag{4.51}
\end{aligned}$$

Combining (4.48)–(4.51), we have the following estimate

$$\begin{aligned}\eta_4 &\leq Ch^k \left(\max_{E \in \Omega_h} \|E\|_{k-1, \infty, E} \|\mathbf{u}\|_{k+1, \Omega} \|\psi\|_{k+1, \Omega} + \|\mathbf{u}\|_{k+1, \Omega} \|\psi\|_{2, \Omega} + \|\psi\|_{k+1, \Omega} \right) \| | | | (\mathbf{v}_h, q_h) | | | \\ &\quad + E^* C_{1 \rightarrow 4}^2 \|\nabla \mathbf{u}\|_\Omega \|\nabla(\psi_I - \psi_h)\|_\Omega \| | | | (\mathbf{v}_h, q_h) | | | .\end{aligned}\quad (4.52)$$

Step 3. We apply the orthogonality of the projectors, the bound (3.11) and Lemma 4.1:

$$\begin{aligned}\eta_5 &= \sum_{E \in \Omega_h} \left(\int_E \tau_E \nabla p \cdot \nabla q_h dE - \int_E \tau_E \Pi_{k-1}^{0,E} \nabla p_I \cdot \Pi_{k-1}^{0,E} \nabla q_h dE - \tau_E S_2^E(p_I - \Pi_{k-1}^{\nabla, E} p_I, q_h - \Pi_{k-1}^{\nabla, E} q_h) \right) \\ &= \sum_{E \in \Omega_h} \left(\int_E \tau_E (\nabla p_I - \Pi_{k-1}^{0,E} \nabla p_I) \cdot \nabla q_h dE - \tau_E S_2^E(p_I - \Pi_{k-1}^{\nabla, E} p_I, q_h - \Pi_{k-1}^{\nabla, E} q_h) \right) \\ &\leq Ch^k \|p\|_{k, \Omega} \| | | | (\mathbf{v}_h, q_h) | | | .\end{aligned}\quad (4.53)$$

Step 4. Concerning η_6 , we proceed as follows

$$\begin{aligned}\eta_6 &= \sum_{E \in \Omega_h} \tau_E \left(\int_E (-\mu \Delta \mathbf{u} + (\mathbf{u} \cdot \nabla \psi) \mathbf{E}) \cdot \nabla q_h dE \right. \\ &\quad \left. - \int_E (-\mu \nabla \cdot \Pi_{k-1}^{0,E} \nabla \mathbf{u}_I + (\Pi_k^{0,E} \mathbf{u}_I \cdot \Pi_{k-1}^{0,E} \nabla \psi) \mathbf{E}) \cdot \Pi_{k-1}^{0,E} \nabla q_h dE \right) \\ &= \sum_{E \in \Omega_h} \tau_E \left(\int_E \mu \nabla \cdot \Pi_{k-1}^{0,E} \nabla (\mathbf{u}_I - \mathbf{u}) \cdot \Pi_{k-1}^{0,E} \nabla q_h dE + \int_E \mu \Delta \mathbf{u} \cdot (\Pi_{k-1}^{0,E} \nabla q_h - \nabla q_h) dE \right. \\ &\quad \left. + \int_E (\mathbf{u} \cdot \nabla \psi) \mathbf{E} \cdot (\nabla q_h - \Pi_{k-1}^{0,E} \nabla q_h) dE + \int_E ((\mathbf{u} - \Pi_k^{0,E} \mathbf{u}_I) \cdot \nabla \psi) \mathbf{E} \cdot \Pi_{k-1}^{0,E} \nabla q_h dE \right. \\ &\quad \left. + \int_E (\Pi_k^{0,E} \mathbf{u}_I \cdot (\nabla \psi - \Pi_{k-1}^{0,E} \nabla \psi_I)) \mathbf{E} \cdot \Pi_{k-1}^{0,E} \nabla q_h dE \right. \\ &\quad \left. + \int_E (\Pi_k^{0,E} \mathbf{u}_I \cdot \Pi_{k-1}^{0,E} \nabla (\psi_I - \psi_h)) \mathbf{E} \cdot \Pi_{k-1}^{0,E} \nabla q_h dE \right) \\ &=: \eta_{6,1} + \eta_{6,2} + \eta_{6,3} + \eta_{6,4} + \eta_{6,5} + \eta_{6,6}.\end{aligned}\quad (4.54)$$

• We use the inverse inequality, definition of $\| | | | \cdot | | | |$, and Lemma 4.2:

$$\eta_{6,1} \leq \sum_{E \in \Omega_h} \tau_E C_{inv} h_E^{-1} \|\nabla(\mathbf{u} - \mathbf{u}_I)\|_E \|\Pi_{k-1}^{0,E} \nabla q_h\|_E \leq Ch^k \|\mathbf{u}\|_{k+1, \Omega} \| | | | (\mathbf{v}_h, q_h) | | | .\quad (4.55)$$

• Recalling the orthogonality of the projectors, definition of τ_E and Lemma 4.1, we have

$$\begin{aligned}\eta_{6,2} &\leq \sum_{E \in \Omega_h} \mu \tau_E \|\Delta \mathbf{u} - \Pi_{k-1}^{0,E} \Delta \mathbf{u}\|_E \|\Pi_{k-1}^{0,E} \nabla q_h - \nabla q_h\|_E \leq \sum_{E \in \Omega_h} \mu \tau_E h_E^{k-1} \|\mathbf{u}\|_{k+1, E} \|\nabla(I - \Pi_{k-1}^{\nabla, E}) q_h\|_E \\ &\leq Ch^k \|\mathbf{u}\|_{k+1, \Omega} \| | | | (\mathbf{v}_h, q_h) | | | .\end{aligned}\quad (4.56)$$

• Following the estimation of $\eta_{6,2}$ and introducing the Sobolev embedding theorem, we arrive at

$$\begin{aligned}\eta_{6,3} &\leq \sum_{E \in \Omega_h} \tau_E \|(\mathbf{u} \cdot \nabla \psi) \mathbf{E} - \Pi_{k-1}^{0,E} ((\mathbf{u} \cdot \nabla \psi) \mathbf{E})\|_E \|\nabla q_h - \Pi_{k-1}^{0,E} \nabla q_h\|_E \\ &\leq \sum_{E \in \Omega_h} \tau_E h_E^{k-1} \|\mathbf{E}\|_{k-1, \infty, E} |\mathbf{u} \cdot \nabla \psi|_{k-1, E} \|\nabla(I - \Pi_{k-1}^{\nabla, E}) q_h\|_E \\ &\leq Ch^k \max_{E \in \Omega_h} \|\mathbf{E}\|_{k-1, \infty, E} \|\mathbf{u}\|_{k+1, \Omega} \|\psi\|_{k+1, \Omega} \| | | | (\mathbf{v}_h, q_h) | | | .\end{aligned}\quad (4.57)$$

- Following the estimation of η_{42} , we infer

$$\eta_{6,4} \leq Ch^k \|\psi\|_{2,\Omega} \|\mathbf{u}\|_{k+1,\Omega} |||(\mathbf{v}_h, q_h)|||. \quad (4.58)$$

- Applying the Sobolev embedding theorem, polynomial inverse inequality, and Lemma 4.1, it holds

$$\begin{aligned} \eta_{6,5} &\leq \sum_{E \in \Omega_h} \tau_E \|\mathbf{u}_I\|_{0,4,E} \|\nabla \psi - \boldsymbol{\Pi}_{k-1}^{0,E} \nabla \psi_I\|_E \|\boldsymbol{\Pi}_{k-1}^{0,E} \nabla q_h\|_{0,4,E} \\ &\leq \sum_{E \in \Omega_h} \tau_E \|\mathbf{u}_I\|_{0,4,E} (\|\nabla \psi - \boldsymbol{\Pi}_{k-1}^{0,E} \nabla \psi\|_E + \|\nabla(\psi - \psi_I)\|_E) h_E^{-1/2} \|\boldsymbol{\Pi}_{k-1}^{0,E} \nabla q_h\|_E \\ &\leq Ch^k \|\nabla \mathbf{u}\|_\Omega \|\psi\|_{k+1,\Omega} |||(\mathbf{v}_h, q_h)||| \\ &\leq Ch^k \|\psi\|_{k+1,\Omega} |||(\mathbf{v}_h, q_h)|||. \end{aligned} \quad (4.59)$$

- Recalling the bound (4.5), Remark 3.2 and the Sobolev embedding theorem, we obtain

$$\begin{aligned} \eta_{6,6} &\leq \sum_{E \in \Omega_h} E^* \tau_E \|\mathbf{u}_I\|_{0,4,E} \|\boldsymbol{\Pi}_{k-1}^{0,E} \nabla(\psi_I - \psi_h)\|_{0,4,E} \|\boldsymbol{\Pi}_{k-1}^{0,E} \nabla q_h\|_E \\ &\leq \sum_{E \in \Omega_h} E^* \tau_E^{1/2} C_{inv} h_E^{-1} \|\mathbf{u}_I\|_{0,4,E} \|\psi_I - \psi_h\|_{0,4,E} |||(\mathbf{v}_h, q_h)|||_E \\ &\leq \frac{E^*}{4} \|\mathbf{u}_I\|_{0,4,\Omega} \|\psi_I - \psi_h\|_{0,4,\Omega} |||(\mathbf{v}_h, q_h)||| \\ &\leq \frac{E^* C_{1 \leftrightarrow 4}^2}{4} \|\nabla \mathbf{u}\|_\Omega \|\nabla(\psi_I - \psi_h)\|_\Omega |||(\mathbf{v}_h, q_h)|||. \end{aligned} \quad (4.60)$$

Adding the estimates (4.55)–(4.60), we arrive at

$$\begin{aligned} \eta_6 &\leq Ch^k (\|\mathbf{u}\|_{k+1,\Omega} + \max_{E \in \Omega_h} \|\mathbf{E}\|_{k-1,\infty,E} \|\mathbf{u}\|_{k+1,\Omega} \|\psi\|_{k+1,\Omega} + \|\psi\|_{2,\Omega} \|\mathbf{u}\|_{k+1,\Omega} + \|\psi\|_{k+1,\Omega}) |||(\mathbf{v}_h, q_h)||| \\ &\quad + \frac{E^* C_{1 \leftrightarrow 4}^2}{4} \|\nabla \mathbf{u}\|_\Omega \|\nabla(\psi_I - \psi_h)\|_\Omega |||(\mathbf{v}_h, q_h)|||. \end{aligned} \quad (4.61)$$

Step 5. Recalling the bound (3.10), the divergence-free property of \mathbf{u} and Lemmas 4.1 and 4.2:

$$\begin{aligned} \eta_7 &= \sum_{E \in \Omega_h} \delta_E \left(\int_E \boldsymbol{\Pi}_{k-1}^{0,E} \nabla \cdot \mathbf{u}_I \boldsymbol{\Pi}_{k-1}^{0,E} \nabla \cdot \mathbf{v}_h dE + S_1^E (\mathbf{u}_I - \boldsymbol{\Pi}_k^{\nabla,E} \mathbf{u}_I, \mathbf{v}_h - \boldsymbol{\Pi}_k^{\nabla,E} \mathbf{v}_h) \right) \\ &= \sum_{E \in \Omega_h} \delta_E \left(\int_E \boldsymbol{\Pi}_{k-1}^{0,E} (\nabla \cdot \mathbf{u}_I - \nabla \cdot \mathbf{u}) \boldsymbol{\Pi}_{k-1}^{0,E} \nabla \cdot \mathbf{v}_h dE + S_1^E (\mathbf{u}_I - \boldsymbol{\Pi}_k^{\nabla,E} \mathbf{u}_I, \mathbf{v}_h - \boldsymbol{\Pi}_k^{\nabla,E} \mathbf{v}_h) \right) \\ &\leq C \sum_{E \in \Omega_h} \delta_E^{1/2} \left(\|\boldsymbol{\Pi}_{k-1}^{0,E} (\nabla \cdot \mathbf{u}_I - \nabla \cdot \mathbf{u})\|_{0,E} + \lambda_1^* \|\nabla(\mathbf{I} - \boldsymbol{\Pi}_k^{\nabla,E}) \mathbf{u}_I\|_{0,E} \right) |||(\mathbf{v}_h, q_h)|||_E \\ &\leq Ch^k \|\mathbf{u}\|_{k+1,\Omega} |||(\mathbf{v}_h, q_h)|||. \end{aligned} \quad (4.62)$$

Finally, combining the estimates (4.46), (4.52), (4.53), (4.61), we obtain the estimate (4.44). \square

Lemma 4.12. *Under the hypothesis of Lemma 4.11, for $(\mathbf{v}_h, q_h) \in \mathbf{V}^h \times Q^h$, the following holds*

$$\begin{aligned}
|F_{PSPG,h}^{\psi_h}(\mathbf{v}_h, q_h) - F_{PSPG}^{\psi}(\mathbf{v}_h, q_h)| &\leq Ch^k \left(\max_{E \in \Omega_h} \|\mathbf{E}\|_{k-1,\infty,E} (\|g\|_{k-1,\Omega} + \|\kappa\|_{k-1,\Omega}) + \|\psi\|_{k+1,\Omega} \right. \\
&\quad \left. \|\mathbf{f}\|_{k-1,\Omega} \right) |||(\mathbf{v}_h, q_h)||| \\
&\quad \left(C_P^2 E^* \kappa^* + \frac{C_P |\Omega|^{1/2} E^* \kappa^*}{4C_{inv}} \right) \|\nabla(\psi_h - \psi_I)\|_{\Omega} |||(\mathbf{v}_h, q_h)|||.
\end{aligned} \tag{4.63}$$

Proof. Let us recall the definition of the loads $F_{PSPG,h}^{\psi_h}(\cdot)$ and $F_{PSPG}^{\psi}(\cdot)$,

$$\begin{aligned}
\eta_F &:= F_{PSPG,h}^{\psi_h}(\mathbf{v}_h, q_h) - F_{PSPG}^{\psi}(\mathbf{v}_h, q_h) \\
&= \sum_{E \in \Omega_h} \left(\int_E \mathbf{\Pi}_k^{0,E} \mathbf{f} \cdot \mathbf{\Pi}_k^{0,E} \mathbf{v}_h \, dE - \int_E \mathbf{f} \cdot \mathbf{v}_h \, dE + \int_E \tau_E \mathbf{\Pi}_k^{0,E} \mathbf{f} \cdot \mathbf{\Pi}_{k-1}^{0,E} \nabla q_h \, dE - \int_E \tau_E \mathbf{f} \cdot \nabla q_h \, dE + \right. \\
&\quad \left. \int_E (g - \kappa(\Pi_k^{0,E} \psi_h)) \mathbf{E} \cdot \mathbf{\Pi}_k^{0,E} \mathbf{v}_h \, dE - \int_E (g - \kappa(\psi)) \mathbf{E} \cdot \mathbf{v}_h \, dE + \right. \\
&\quad \left. \int_E \tau_E (g - \kappa(\Pi_k^{0,E} \psi_h)) \mathbf{E} \cdot \mathbf{\Pi}_{k-1}^{0,E} \nabla q_h \, dE - \int_E \tau_E (g - \kappa(\psi)) \mathbf{E} \cdot \nabla q_h \, dE \right) \\
&=: \eta_{F,1} + \eta_{F,2} + \eta_{F,3} + \eta_{F,4}.
\end{aligned} \tag{4.64}$$

Employing the orthogonality of the projection operators, regularity **(A2)** and Lemma 4.1, we infer

$$\begin{aligned}
\eta_{F,1} &= \sum_{E \in \Omega_h} \int_E (\mathbf{\Pi}_k^{0,E} \mathbf{f} - \mathbf{f}) \cdot (\mathbf{v}_h - \mathbf{\Pi}_k^{0,E} \mathbf{v}_h) \, dE \leq \sum_{E \in \Omega_h} \|\mathbf{\Pi}_k^{0,E} \mathbf{f} - \mathbf{f}\|_E \|\mathbf{v}_h - \mathbf{\Pi}_k^{0,E} \mathbf{v}_h\|_E \\
&\leq Ch^k \|\mathbf{f}\|_{k-1,\Omega} |||(\mathbf{v}_h, q_h)|||.
\end{aligned} \tag{4.65}$$

Following the estimation of $\eta_{F,1}$, and using the definition of τ_E and $||| \cdot |||$, it holds

$$\eta_{F,2} \leq Ch^k \|\mathbf{f}\|_{k-1,\Omega} |||(\mathbf{v}_h, q_h)|||. \tag{4.66}$$

Concerning $\eta_{F,3}$, we add and subtract suitable terms, and use the property of the projectors and

Lemma 4.1:

$$\begin{aligned}
\eta_{F,3} &= \sum_{E \in \Omega_h} \left(\int_E (g - \kappa(\Pi_k^{0,E} \psi_h)) \mathbf{E} \cdot \mathbf{\Pi}_k^{0,E} \mathbf{v}_h \, dE - \int_E (g - \kappa(\psi)) \mathbf{E} \cdot \mathbf{v}_h \, dE \right) \\
&= \sum_{E \in \Omega_h} \left(\int_E g \mathbf{E} \cdot (\mathbf{\Pi}_k^{0,E} \mathbf{v}_h - \mathbf{v}_h) \, dE + \int_E (\kappa(\psi) - \kappa(\Pi_k^{0,E} \psi_h)) \mathbf{E} \cdot \mathbf{\Pi}_k^{0,E} \mathbf{v}_h \, dE \right. \\
&\quad \left. + \int_E \kappa(\psi) \mathbf{E} \cdot (\mathbf{v}_h - \mathbf{\Pi}_k^{0,E} \mathbf{v}_h) \, dE \right) \\
&= \sum_{E \in \Omega_h} \left(\int_E (g \mathbf{E} - \mathbf{\Pi}_k^{0,E} (g \mathbf{E})) \cdot (\mathbf{\Pi}_k^{0,E} \mathbf{v}_h - \mathbf{v}_h) \, dE + \int_E (\kappa(\psi) - \kappa(\Pi_k^{0,E} \psi_h)) \mathbf{E} \cdot \mathbf{\Pi}_k^{0,E} \mathbf{v}_h \, dE \right. \\
&\quad \left. + \int_E (\kappa(\psi) \mathbf{E} - \mathbf{\Pi}_k^{0,E} (\kappa(\psi) \mathbf{E})) \cdot (\mathbf{v}_h - \mathbf{\Pi}_k^{0,E} \mathbf{v}_h) \, dE \right) \\
&\leq C \sum_{E \in \Omega_h} \left(h_E^k \|\mathbf{E}\|_{k-1,\infty,E} \|g\|_{k-1,E} \|\nabla \mathbf{v}_h\|_E + E^* \kappa^* \|\psi - \Pi_k^{0,E} \psi_h\|_E \|\mathbf{v}_h\|_E \right. \\
&\quad \left. + h_E^k \|\mathbf{E}\|_{k-1,\infty,E} \|\kappa\|_{k-1,E} \|\nabla \mathbf{v}_h\|_E \right) \\
&\leq C h^k \left(\max_{E \in \Omega_h} \|\mathbf{E}\|_{k-1,\infty,E} (\|g\|_{k-1,\Omega} + \|\kappa\|_{k-1,\Omega}) + \|\psi\|_{k+1,\Omega} \right) \|\|(\mathbf{v}_h, q_h)\| \| \\
&\quad + C_P^2 E^* \kappa^* \|\nabla(\psi_h - \psi_I)\|_\Omega \|\|(\mathbf{v}_h, q_h)\| \|. \tag{4.67}
\end{aligned}$$

Following the estimation of $\eta_{F,3}$ and using the definition of τ_E , we arrive at

$$\begin{aligned}
\eta_{F,4} &\leq C h^k \left(\max_{E \in \Omega_h} \|\mathbf{E}\|_{k-1,\infty,E} (\|g\|_{k,\Omega} + \|\kappa\|_{k-1,\Omega}) + \|\psi\|_{k+1,\Omega} \right) \|\|(\mathbf{v}_h, q_h)\| \| \\
&\quad + \frac{C_P |\Omega|^{1/2} E^* \kappa^*}{4 C_{inv}} \|\nabla(\psi_h - \psi_I)\|_\Omega \|\|(\mathbf{v}_h, q_h)\| \|,
\end{aligned} \tag{4.68}$$

which completes the proof. \square

Lemma 4.13. *Let the assumption (A2) and the hypothesis of Theorems 2.2 and 4.7 hold true. For any given $\mathbf{u} \in \mathbf{V}_{div}$ and $\mathbf{u}_h \in \mathbf{V}^h$, let $\psi \in \Phi$ and $\psi_h \in \phi_h$ be the solution of problems (2.8) and (3.16), respectively. Then, the following holds*

$$\begin{aligned}
\|\nabla(\psi_I - \psi_h)\|_\Omega &\leq C h^k \left(\|\psi\|_{k+1,\Omega} + \|\mathbf{u}\|_{k+1,\Omega} + \|\psi\|_{k+1,\Omega} \|\mathbf{u}\|_{k,\Omega} + \|\kappa\|_{k-1,\Omega} + \|g\|_{k-1,\Omega} \right) \\
&\quad + \frac{C_{1 \leftrightarrow 4}^2}{\gamma_* \epsilon} \|\nabla \psi\|_\Omega \|\nabla(\mathbf{u}_I - \mathbf{u}_h)\|_\Omega. \tag{4.69}
\end{aligned}$$

Proof. We first set $\tilde{\phi}_h := \psi_I - \psi_h$, and let us recall the stability properties of the bilinear form $a_p(\cdot, \cdot)$ and $a_{p,h}(\cdot, \cdot)$ and the strongly monotone property of $\kappa(\cdot)$, we infer

$$\begin{aligned}
\gamma_* \epsilon \|\nabla(\psi_I - \psi_h)\|_\Omega^2 &\leq \mathcal{B}_h(\mathbf{u}_h; \psi_h, \tilde{\phi}_h) - \mathcal{B}(\mathbf{u}_h; \psi_I, \tilde{\phi}_h) \\
&= (g_h, \tilde{\phi}_h) - (g, \tilde{\phi}_h) + \mathcal{B}(\mathbf{u}; \psi, \tilde{\phi}_h) - \mathcal{B}(\mathbf{u}_h; \psi_I, \tilde{\phi}_h) \\
&= (g_h, \tilde{\phi}_h) - (g, \tilde{\phi}_h) + a_p(\psi, \tilde{\phi}_h) - a_{p,h}(\psi_I, \tilde{\phi}_h) + c_p^{skew}(\mathbf{u}; \psi, \tilde{\phi}_h) - c_{p,h}^{skew}(\mathbf{u}_h; \psi_I, \tilde{\phi}_h) \\
&\quad + a_d(\psi, \tilde{\phi}_h) - a_d(\psi_I, \tilde{\phi}_h) \\
&=: b_0 + b_1 + b_2 + b_3. \tag{4.70}
\end{aligned}$$

- Employing the orthogonality of $\Pi_k^{0,E}$, the assumption **(A2)** and Lemma 4.1, we have

$$b_0 \leq \sum_{E \in \Omega_h} \|g - \Pi_k^{0,E} g\|_E \|\tilde{\phi}_h - \Pi_k^{0,E} \tilde{\phi}_h\|_E \leq Ch^k \|g\|_{k-1,\Omega} \|\nabla \tilde{\phi}_h\|_\Omega. \quad (4.71)$$

- We use the triangle inequality, the property of L^2 -projectors, the bound (3.13) and Lemmas 4.1 and 4.2:

$$\begin{aligned} b_1 &= \sum_{E \in \Omega_h} \epsilon \left(\int_E \nabla \psi \cdot \nabla \tilde{\phi}_h \, dE - \int_E \mathbf{\Pi}_{k-1}^{0,E} \nabla \psi_I \cdot \mathbf{\Pi}_{k-1}^{0,E} \nabla \tilde{\phi}_h \, dE - S_3^E(\psi_I - \Pi_k^{\nabla,E} \psi_I, \tilde{\phi}_h - \Pi_k^{\nabla,E} \tilde{\phi}_h) \right) \\ &= \sum_{E \in \Omega_h} \epsilon \left(\int_E (\nabla \psi - \mathbf{\Pi}_{k-1}^{0,E} \nabla \psi_I) \cdot \mathbf{\Pi}_{k-1}^{0,E} \nabla \tilde{\phi}_h \, dE - S_3^E(\psi_I - \Pi_k^{\nabla,E} \psi_I, \tilde{\phi}_h - \Pi_k^{\nabla,E} \tilde{\phi}_h) \right) \\ &\leq C \sum_{E \in \Omega_h} \epsilon \left(h_E^k \|\psi\|_{k+1,E} \|\nabla \tilde{\phi}_h\|_E + \lambda_3^* h_E^k \|\psi\|_{k+1,E} \|\nabla \tilde{\phi}_h\|_E \right) \\ &\leq Ch^k \|\psi\|_{k+1,\Omega} \|\nabla \tilde{\phi}_h\|_\Omega. \end{aligned} \quad (4.72)$$

- Concerning b_2 , we proceed as follows

$$\begin{aligned} b_2 &= c_p^{skew}(\mathbf{u}; \psi, \tilde{\phi}_h) - c_{p,h}^{skew}(\mathbf{u}_h; \psi_I, \tilde{\phi}_h) \\ &= c_p^{skew}(\mathbf{u}; \psi, \tilde{\phi}_h) - c_{p,h}^{skew}(\mathbf{u}; \psi, \tilde{\phi}_h) + c_{p,h}^{skew}(\mathbf{u} - \mathbf{u}_h; \psi, \tilde{\phi}_h) + c_{p,h}^{skew}(\mathbf{u}_h; \psi - \psi_I, \tilde{\phi}_h) \\ &=: b_{2,1} + b_{2,2} + b_{2,3}. \end{aligned} \quad (4.73)$$

Following [17, Lemma 4.3], there holds that

$$\begin{aligned} |b_{2,1}| &\leq Ch^k \left(\|\mathbf{u}\|_{k,\Omega} \|\psi\|_{k+1,\Omega} + \|\nabla \mathbf{u}\|_\Omega \|\psi\|_{k+1,\Omega} + \|\mathbf{u}\|_{k+1,\Omega} \|\nabla \psi\|_\Omega \right) \|\nabla \tilde{\phi}_h\|_\Omega \\ &\leq Ch^k \left(\|\mathbf{u}\|_{k,\Omega} \|\psi\|_{k+1,\Omega} + \|\psi\|_{k+1,\Omega} + \|\mathbf{u}\|_{k+1,\Omega} \right) \|\nabla \tilde{\phi}_h\|_\Omega. \end{aligned} \quad (4.74)$$

We use the Sobolev embedding theorem and the estimation of η_{43} :

$$|b_{2,2}| \leq C_{1 \rightarrow 4}^2 \|\nabla(\mathbf{u} - \mathbf{u}_h)\|_\Omega \|\nabla \psi\|_\Omega \|\nabla \tilde{\phi}_h\|_\Omega. \quad (4.75)$$

Following the estimation of η_{43} , we get

$$\begin{aligned} |b_{2,3}| &\leq Ch^k \|\nabla \mathbf{u}_h\|_\Omega \|\psi\|_{k+1,\Omega} \|\nabla \tilde{\phi}_h\|_\Omega \\ &\leq Ch^k \|\psi\|_{k+1,\Omega} \|\nabla \tilde{\phi}_h\|_\Omega, \end{aligned} \quad (4.76)$$

where the last line is obtained using the boundedness of \mathbf{u}_h in the H^1 -semi norm.

Combining the estimates (4.74)–(4.75) and applying Lemma 4.2, we obtain the following

$$\begin{aligned} b_2 &\leq Ch^k \left((1 + \|\mathbf{u}\|_{k,\Omega}) \|\psi\|_{k+1,\Omega} + \|\mathbf{u}\|_{k+1,\Omega} \right) \|\nabla \tilde{\phi}_h\|_\Omega \\ &\quad + C_{1 \rightarrow 4}^2 \|\nabla(\mathbf{u}_I - \mathbf{u}_h)\|_\Omega \|\nabla \psi\|_\Omega \|\nabla \tilde{\phi}_h\|_\Omega. \end{aligned} \quad (4.77)$$

- Adding and subtracting appropriate terms and using the orthogonality property of $\Pi_k^{0,E}$, we infer

$$\begin{aligned}
b_3 &= \sum_{E \in \Omega_h} \left(\int_E \kappa(\psi) \tilde{\phi}_h dE - \int_E \kappa(\Pi_k^{0,E} \psi_I) \Pi_k^{0,E} \tilde{\phi}_h dE \right) \\
&= \sum_{E \in \Omega_h} \left(\int_E (\kappa(\psi) - \Pi_k^{0,E} \kappa(\psi)) (\tilde{\phi}_h - \Pi_k^{0,E} \tilde{\phi}_h) dE - \int_E (\kappa(\psi) - \kappa(\Pi_k^{0,E} \psi_I)) \Pi_k^{0,E} \tilde{\phi}_h dE \right) \\
&\leq C \sum_{E \in \Omega_h} \left(h_E^k \|\kappa(\psi)\|_{k-1,E} \|\nabla \tilde{\phi}_h\|_E + \kappa^* \|\psi - \Pi_k^{0,E} \psi_I\|_E \|\tilde{\phi}_h\|_E \right) \\
&\leq Ch^k \left(\|\kappa\|_{k-1,\Omega} + \|\psi\|_{k+1,\Omega} \right) \|\nabla \tilde{\phi}_h\|_\Omega.
\end{aligned} \tag{4.78}$$

Finally, combining the estimates (4.71), (4.72), (4.77) and (4.78), we readily arrive at the result (4.69). \square

Hereafter, we present the convergence estimate in the energy norm:

Proposition 4.14. *Under the assumption **(A0)** and the assumptions of Proposition 2.5 and Proposition 4.10, let $(\mathbf{u}, p, \psi) \in \mathbf{V} \times Q \times \Phi$ and $(\mathbf{u}_h, p_h, \psi_h) \in \mathbf{V}^h \times Q^h \times \phi_h$ be the solution of the problems (2.7) and (3.14). Furthermore, we assume that the stabilization parameters are such that the assumption (4.11) holds true. We assume that data of problem (2.1) are such that*

$$\beta_* - \frac{\mu}{2\gamma_*\epsilon} \left(\frac{5C_{1\leftarrow 4}^2}{4} C_u + C_P^2 \kappa^* + \frac{C_P |\Omega|^{1/2} \kappa^*}{4C_{inv}} \right) > 0. \tag{4.79}$$

Then under the assumption **(A2)**, we have the following error estimate

$$\begin{aligned}
\| | | | (\mathbf{u} - \mathbf{u}_h, p - p_h) | | | + \|\nabla(\theta - \theta_h)\|_\Omega &\leq Ch^k \left(\|\mathbf{u}\|_{k+1,\Omega} + \|p\|_{k,\Omega} + \|\psi\|_{k+1,\Omega} + \|\mathbf{u}\|_{k+1,\Omega} \|\psi\|_{k+1,\Omega} \right. \\
&\quad \left. + \|\psi\|_{2,\Omega} \|\mathbf{u}\|_{k+1,\Omega} \|g\|_{k-1,\Omega} + \|\kappa\|_{k-1,\Omega} + \|\psi\|_{k+1,\Omega} + \|\mathbf{f}\|_{k-1,\Omega} \right),
\end{aligned} \tag{4.80}$$

where the positive constant C additionally depends on \mathbf{E} .

Proof. Using the discrete inf-sup condition (4.12), it holds

$$\begin{aligned}
\beta_* \| | | | (\mathbf{u}_h - \mathbf{u}_I, p_h - p_I) | | | \| | | | (\mathbf{v}_h, q_h) | | | &\leq \mathcal{A}_{\text{PSPG},h}(\psi_h; (\mathbf{u}_h - \mathbf{u}_I, p_h - p_I), (\mathbf{v}_h, q_h)) \\
&= F_{\text{PSPG},h}^{\psi_h}(\mathbf{v}_h, q_h) - F_{\text{PSPG}}^{\psi}(\mathbf{v}_h, q_h) \\
&\quad + \mathcal{A}_{\text{PSPG}}(\psi; (\mathbf{u}, p), (\mathbf{v}_h, q_h)) - \mathcal{A}_{\text{PSPG},h}(\psi_h; (\mathbf{u}_I, p_I), (\mathbf{v}_h, q_h)) \\
&=: \eta_F + \eta_A.
\end{aligned} \tag{4.81}$$

Recalling Lemmas 4.11 and 4.12, we have

$$\begin{aligned}
\beta_* \| | | | (\mathbf{u}_h - \mathbf{u}_I, p_h - p_I) | | | &\leq Ch^k \left(\|\mathbf{u}\|_{k+1,\Omega} + \|p\|_{k,\Omega} + \|\psi\|_{k+1,\Omega} + \|\mathbf{u}\|_{k+1,\Omega} \|\psi\|_{k+1,\Omega} + \|\psi\|_{2,\Omega} \|\mathbf{u}\|_{k+1,\Omega} \right. \\
&\quad \left. \|g\|_{k-1,\Omega} + \|\kappa\|_{k-1,\Omega} + \|\psi\|_{k+1,\Omega} + \|\mathbf{f}\|_{k-1,\Omega} \right) \\
&\quad + \left(\frac{5E^* C_{1\leftarrow 4}^2}{4} \|\nabla \mathbf{u}\|_\Omega + C_P^2 E^* \kappa^* + \frac{C_P |\Omega|^{1/2} E^* \kappa^*}{4C_{inv}} \right) \|\nabla(\psi_h - \psi_I)\|_\Omega.
\end{aligned} \tag{4.82}$$

Employing Lemma 4.13, the Sobolev embedding theorem and the assumption (4.79), yields

$$\| |(\mathbf{u}_h - \mathbf{u}_I, p_h - p_I)| \| \leq Ch^k \left(\|\mathbf{u}\|_{k+1,\Omega} + \|p\|_{k,\Omega} + \|\psi\|_{k+1,\Omega} + \|\mathbf{u}\|_{k+1,\Omega} \|\psi\|_{k+1,\Omega} + \|\psi\|_{2,\Omega} \|\mathbf{u}\|_{k+1,\Omega} \right. \\ \left. \|g\|_{k-1,\Omega} + \|\kappa\|_{k-1,\Omega} + \|\psi\|_{k+1,\Omega} + \|\mathbf{f}\|_{k-1,\Omega} \right). \quad (4.83)$$

Thus, the estimate (4.80) can be easily obtained by combining the estimates (4.83) and (4.69) and the interpolant estimate (4.3). \square

4.4. Discussion of the smallness condition

The convergence estimate of Proposition 4.14 requires condition (4.79), which demands that the discrete inf-sup constant β_* be strictly larger than a quantity that depends on the viscosity μ , the permittivity ϵ , the nonlinearity parameter κ^* , the velocity bound C_u , the Poincaré constant C_P , the Sobolev embedding constant $C_{1 \rightarrow 4}$, and the inverse inequality constant C_{inv} . In this subsection, we discuss the origin, the practical restrictiveness, and the indirect numerical verification of this condition.

The error analysis of the coupled Stokes-Poisson-Boltzmann system introduces a cross-coupling between the velocity-pressure error and the potential error. Specifically, the Stokes error bound (cf. the estimate preceding (4.83)) contains a term proportional to $\|\nabla(\psi_h - \psi_I)\|_\Omega$, arising from the dependence of the Stokes bilinear form on the potential field. Through Lemma 4.13, this potential error in turn depends on the velocity error $\|\nabla(\mathbf{u}_I - \mathbf{u}_h)\|_\Omega$, creating a feedback loop. Condition (4.79) ensures that the coupling coefficient is strictly smaller than β_* , so that the feedback can be resolved and the velocity-pressure error can be bounded purely in terms of interpolation errors.

Smallness conditions of this type are a standard feature of the analysis of nonlinearly coupled systems. In the finite element analysis of the same Stokes-Poisson-Boltzmann model, AlSohaim et al. [2] require three analogous conditions [2, conditions (2.11), (2.12), and (3.3)], involving generic Sobolev and stability constants that are likewise not explicitly computable in closed form. Similar assumptions appear in the analysis of stabilized methods for related coupled problems [33, 34]. In all these references, the conditions are stated as abstract inequalities and verified only indirectly through the numerical experiments.

Although condition (4.79) cannot be verified algebraically for specific parameter values (due to the presence of generic constants such as β_* and C_{inv}), its dependence on the physical parameters can be interpreted qualitatively. The subtracted quantity in (4.79) scales as $\mu/(\gamma_* \epsilon)$ times a combination of C_u and κ^* . Therefore, the condition becomes more restrictive when:

- (i) the ratio μ/ϵ is large, corresponding to regimes where viscous effects dominate over electrostatic screening;
- (ii) the nonlinearity strength κ^* is large, which occurs when the ionic activity coefficients α_0 and α_1 produce strong charge densities;
- (iii) the velocity bound C_u is large, which by (2.9) happens when the external forces \mathbf{f} and the source term g are large relative to the viscosity.

Conversely, the condition is more easily satisfied for moderate physical parameters and small data.

For the parameter regimes considered in the numerical experiments of Section 6, several factors contribute to the expectation that condition (4.79) is satisfied with a comfortable margin. In Example 5.1, the moderate parameter values $\mu = 1$, $\kappa = 1$, $\alpha_0 = \alpha_1 = 1$, and $\mathbf{E} = [0, -1]^T$ yield a regime where the coupling effects are mild. In Example 5.3, although $\mu/\epsilon = 0.1/0.075 \approx 1.33$ is

not particularly small, the very small ionic activity coefficient $\alpha_0 = 0.001$ produces a correspondingly small nonlinearity parameter κ^* , significantly reducing the subtracted quantity in (4.79). The numerical experiments provide two forms of indirect evidence that the condition holds. First, the fixed-point iteration converges consistently within 7–8 iterations across all mesh sizes and polynomial orders $k = 1$ and $k = 2$, with no sign of deterioration under mesh refinement. Second, the computed convergence rates closely match the theoretical prediction $\mathcal{O}(h^k)$ on all mesh types, including non-convex polygons and meshes with hanging nodes. If condition (4.79) were violated or only marginally satisfied, one would expect either divergence of the fixed-point scheme, degradation of convergence rates on finer meshes, or sensitivity to the mesh type, none of which is experimentally observed.

5. Numerical results

Hereafter, we investigate the practical behavior of the proposed method (3.14) through three numerical examples that validate the theoretical estimates derived in Section 4.3. In these test cases, we consider convex and non-convex domains, including meshes with hanging nodes, demonstrating the geometric flexibility of the proposed method.

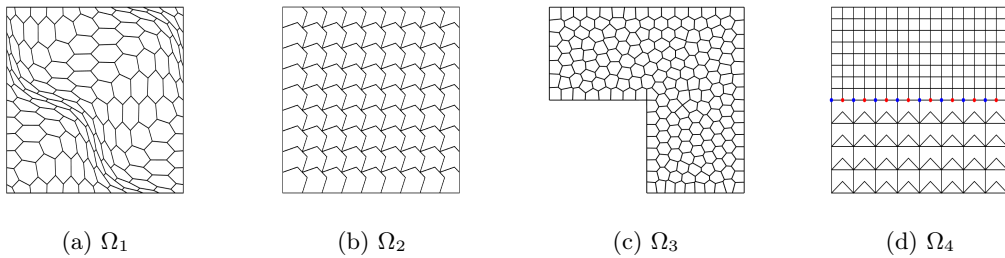


Figure 1: Convex and non-convex domains with general polygons including hanging nodes Ω_4 .

All computations employ VEM orders $k = 1$ and $k = 2$ to confirm optimal convergence for different polynomial degrees, and a fixed-point iterative scheme for solving the nonlinear stabilized virtual element problem (3.14) with stopping threshold equal to 10^{-6} . Following Lemma 4.5, stabilization parameters are chosen as $\tau_E \sim h_E^2$ and $\delta_E \sim h_E$. For domains Ω_1 , Ω_2 , and Ω_4 on the unit square, we employ mesh sizes $h = 1/N$, with $N \in \{5, 10, 20, 40, 80\}$, while the L-shaped domain Ω_3 uses the sequence $N \in \{4, 8, 16, 32, 64\}$. A sample of computational meshes is shown in Figure 1.

We quantify the absolute errors in the $H^1(\Omega)$ semi-norm for the velocity field and the L^2 -norm for the pressure field as follows:

$$E_{H^1}^{\mathbf{u}} := \sqrt{\sum_{E \in \Omega_h} \|\nabla(\mathbf{u} - \boldsymbol{\Pi}_k^{\nabla, E} \mathbf{u}_h)\|_E^2}, \quad E_{L^2}^p := \sqrt{\sum_{E \in \Omega_h} \|p - \boldsymbol{\Pi}_k^{0, E} p_h\|_E^2},$$

where the exact and discrete velocities are denoted by \mathbf{u} and \mathbf{u}_h , and p and p_h for exact and discrete pressure field, and $\boldsymbol{\Pi}_k^{\nabla, E}$ and $\boldsymbol{\Pi}_k^{0, E}$ are the elliptic and L^2 -orthogonal projectors discussed in Section 3.2. Following the above notations, we use $E_{H^1}^{\psi}$ to represent the absolute error in the potential field.

5.1. Example 1: Convergence studies on convex domains

In this first example, we consider a manufactured solution with smooth velocity, pressure, and potential fields to validate optimal convergence rates on various polygonal meshes. The parameters

defining problem 2.1 are:

$$\mu = 1, \quad \kappa = 1, \quad \alpha_0 = \alpha_1 = 1, \quad \mathbf{E} = [0, -1]^T.$$

Let $\xi(x, y) := x^3 y^3 (1-x)^3 (1-y)^3$ define an auxiliary function. Then, we consider the exact solution fields:

$$\begin{cases} \mathbf{u}(x, y) = \left[\frac{d\xi}{dy}, -\frac{d\xi}{dx} \right], \\ p(x, y) = \sin(\pi x) \cos(\pi y) + p_0, \\ \psi(x, y) = x^2 y^2 (x-1)(y-1), \end{cases}$$

where p_0 is the pressure constant ensuring the zero-mean pressure constraint according to (2.2). The load terms and the boundary conditions are derived accordingly.

Tables 1–3 present numerical errors and convergence rates on the unit square using computational meshes Ω_1 (distorted hexagons), Ω_2 (non-convex polygons), and Ω_4 (composite mesh with non-convex polygons and hanging nodes). These numerical results confirm that the stabilized VEM achieves the optimal theoretical convergence rates derived in Section 4.3, which are $\mathcal{O}(h)$ for $k = 1$ and $\mathcal{O}(h^2)$ for $k = 2$ for the three solution fields, i.e., velocity, pressure and potential.

Additionally, we remark that the meshes of the mesh family Ω_4 are constructed through the composition of two non-matching meshes, thus leading to hanging nodes at the shared interface. Table 3 shows that optimal convergence is maintained without special treatment of these hanging nodes, confirming that this method naturally handles possible mesh non-conformities.

Table 1: [Example 1] Convergence studies on distorted hexagons Ω_1 using proposed method

order	h	$E_{H^1}^{\mathbf{u}}$	rate	$E_{L^2}^p$	rate	$E_{H^1}^{\psi}$	rate	itr
k=1	1/5	1.311720e-02	–	2.449411e-02	–	8.705857e-03	–	7
	1/10	6.428537e-03	1.029	1.221762e-02	1.004	4.577561e-03	0.927	7
	1/20	3.232437e-03	0.992	6.103906e-03	1.001	2.345729e-03	0.965	7
	1/40	1.623956e-03	0.993	3.052641e-03	1.000	1.187052e-03	0.983	7
	1/80	8.136887e-04	0.997	1.527061e-03	0.999	5.970562e-04	0.991	8
k=2	1/5	2.681120e-02	–	4.503502e-02	–	8.103336e-04	–	7
	1/10	6.049456e-03	2.418	1.181225e-02	1.931	2.221737e-04	1.867	7
	1/20	1.533453e-03	1.980	3.019989e-03	1.968	5.772350e-05	1.945	7
	1/40	3.893513e-04	1.978	7.607732e-04	1.989	1.468018e-05	1.975	7
	1/80	9.810407e-05	1.989	1.910031e-04	1.994	3.699626e-06	1.988	8

5.2. Example 2: Convergence studies on non-convex domain

In this example, we investigate the convergence behavior of the proposed method on the non-convex domain with re-entrant corners for a problem with a known solution. We introduce an L-shaped non-convex domain given by $(0, 1)^2 \setminus (0, 0.5)^2$, discretized with regular Voronoi mesh, as shown in Figure 1(c). We consider the same manufactured solution of Example 1. The problem parameters are the same, with the exception of the pressure p_0 , which must be recalculated for the L-shaped domain by using (2.2).

Table 4 confirms optimal convergence rates $\mathcal{O}(h)$ for $k = 1$ and $\mathcal{O}(h^2)$ for $k = 2$ for the approximation of all fields, velocity, pressure and potential, showing that the geometric non-convexity does not degrade the theoretical convergence behavior. In fact, the Voronoi tessellation maintains the mesh regularity assumption **(A1)** that we introduced at the beginning of Section 3.

Table 2: [Example 1] Convergence studies on non-convex mesh Ω_2 using proposed method

order	h	$E_{H^1}^{\mathbf{u}}$	rate	$E_{L^2}^p$	rate	$E_{H^1}^{\psi}$	rate	itr
k=1	1/5	2.002868e-02	—	3.248449e-02	—	1.051645e-02	—	7
	1/10	8.161245e-03	1.295	1.427017e-02	1.187	5.393170e-03	0.963	7
	1/20	3.621136e-03	1.172	6.640047e-03	1.106	2.730142e-03	0.982	7
	1/40	1.722770e-03	1.072	3.201921e-03	1.052	1.373356e-03	0.991	7
	1/80	8.462576e-04	1.026	1.527061e-03	1.024	6.887283e-04	0.996	8
k=2	1/5	1.434075e-02	—	2.543417e-02	—	1.241960e-03	—	7
	1/10	3.361010e-03	2.093	6.199488e-03	2.034	3.220434e-04	1.947	7
	1/20	8.330459e-04	2.012	1.548879e-03	2.001	8.184041e-05	1.976	7
	1/40	2.077321e-04	2.004	3.889136e-04	1.994	2.061589e-05	1.989	7
	1/80	5.180141e-05	2.004	9.781639e-05	1.991	5.172670e-06	1.995	8

 Table 3: [Example 1] Convergence studies on mesh Ω_4 using proposed method

order	h	$E_{H^1}^{\mathbf{u}}$	rate	$E_{L^2}^p$	rate	$E_{H^1}^{\psi}$	rate	itr
k=1	1/5	1.700467e-02	—	3.324558e-02	—	7.411002e-03	—	7
	1/10	6.418063e-03	1.406	8.366519e-03	1.991	3.720487e-03	0.994	7
	1/20	2.918559e-03	1.137	3.066089e-03	1.448	1.861992e-03	0.999	7
	1/40	1.411469e-03	1.048	1.542844e-03	0.991	9.312391e-04	1.000	7
	1/80	6.982803e-04	1.015	7.846744e-04	0.975	4.656609e-04	1.000	8
k=2	1/5	1.853717e-02	—	3.539204e-02	—	6.973699e-04	—	7
	1/10	4.086304e-03	2.182	7.855160e-03	2.172	1.755867e-04	1.990	7
	1/20	9.677780e-04	2.078	1.888270e-03	2.057	4.397411e-05	1.998	7
	1/40	2.349881e-04	2.042	4.751719e-04	1.991	1.099864e-05	1.999	7
	1/80	5.806576e-05	2.017	1.270720e-04	1.903	2.750029e-06	2.000	8

5.3. Example 3: Flows in nanopore sensor with obstacles

The final example demonstrates the VEM formulation's capability for simulating realistic electrically charged flows in a nanopore sensor with T-shaped and curved-shaped obstacles, which is the same configuration considered in [42, 2]. The geometry and computational meshes are shown in Figure 2 with the sizes 12 nm \times 16 nm (for T-shaped obstacles: (a)) and 12 nm \times 14 nm (for curved shaped obstacles: (b)). An ionic current is driven by an imposed electric potential difference across the nanopore. The electrostatic potential ψ is prescribed on the inflow (bottom) and outflow (top) boundaries as $\psi_{in} = 0$ and $\psi_{out} = 2$, and zero-flux conditions on all other boundaries.

For the velocity field, on the top boundary we impose the parabolic inflow profile

$$\mathbf{u}_{in}(x) = \begin{pmatrix} 0 \\ -0.1 \tanh(40(6-x)^2) \end{pmatrix};$$

and $\mathbf{u} \cdot \mathbf{n} = 0$ on the lateral (right and left) boundaries, zero-traction conditions at the outflow, and no-slip conditions on the obstacle surfaces and channel walls. In this example, we incorporate the nonlinear convective term in the momentum equation. We consider the following parameters

$$\mu = 0.1 \text{ Pa} \cdot \text{s} \quad \epsilon = 0.075, \quad \alpha_0 = 0.001, \quad \alpha_1 = 1, \quad \mathbf{f} = 0, \quad g = 0.$$

Table 4: [Example 2] Convergence studies on L-shaped domain with Voronoi mesh using proposed method

order	h	$E_{H^1}^u$	rate	$E_{L^2}^p$	rate	$E_{H^1}^\psi$	rate	itr
k=1	1/4	5.412799e-03	—	1.761315e-02	—	1.240271e-02	—	5
	1/8	2.089460e-03	1.438	4.781077e-03	1.970	6.441351e-03	0.990	6
	1/16	7.826530e-04	1.485	1.341547e-03	1.921	3.300835e-03	1.011	6
	1/32	3.606618e-04	1.014	5.436234e-04	1.182	1.474711e-03	1.055	6
	1/64	1.644670e-04	1.123	2.656548e-04	1.030	7.382761e-04	0.995	6
k=2	1/4	9.673890e-03	—	2.603108e-02	—	1.745202e-03	—	5
	1/8	1.324590e-03	3.005	6.156831e-03	2.179	4.313425e-04	2.112	6
	1/16	2.939265e-04	2.276	1.583476e-03	2.053	1.094255e-04	2.074	6
	1/32	5.019257e-05	2.314	3.452908e-04	1.994	2.263689e-05	2.062	6
	1/64	1.248291e-05	2.002	9.124393e-05	1.914	5.360583e-06	2.072	7

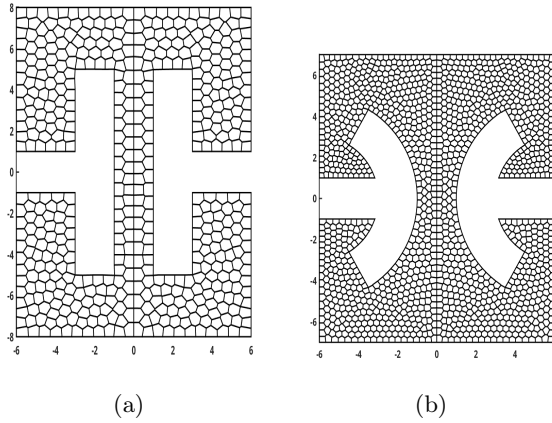


Figure 2: [Example 3] Computational domains with their geometry.

We investigate the practical behavior of the VEM in the two cases with $\mathbf{E} = [0.1, -0.1]^t$ and $\mathbf{E} = [1, -1]^t$. In both cases, we employ a Voronoi mesh with 18,000 elements, and VEM orders $k = 1$ and $k = 2$, and the externally applied electric field \mathbf{E} does not act straight down, but with a slight angle to break symmetry with low and moderate magnitudes. For $\mathbf{E} = [0.1, -0.1]^t$, the stabilized velocity norm, the stabilized pressure, and the potential distribution in the nanopore sensor with T-shaped obstacles are shown in Figures 3 and 4 for VEM order $k = 1$ and $k = 2$. The recirculation region appears near the obstacles due to the combined effects of viscous drag and electrostatic forces. The pressure drop is noticed from the inlet to the outlet. The potential field exhibits smooth gradients from the inflow to outflow boundary, slightly distorted near the obstacles due to the applied electric field. For $k = 1$, we observe a singularity for the velocity field near $(-6, 1)$ and $(6, 1)$, which is effectively suppressed by employing the higher order VEM $k = 2$ as shown in 4. Additionally, the electro-hydrodynamics flow pattern obtained using the proposed method is almost identical to that of [2].

For $\mathbf{E} = [1, -1]^t$, the flow pattern in the nanopore sensor with T-shaped obstacles is shown in Figure 5 for VEM order $k = 2$. We notice that the flow pattern becomes slightly complex as we increase the magnitude of the applied electric field, and the proposed method is efficient in capturing the flow dynamics without exhibiting oscillation or singularities near the corner of the T-shaped obstacles.

The flow dynamics of the electrically charged fluid in the nanopore sensor with curved obstacles are shown in Figure 6 for $E = [0.1, -0.1]^t$ and $\mathbf{E} = [1, -1]^t$ with higher order VEM $k = 2$. We notice that the flow characteristics are similar to the previous case, but becomes slightly complex as we increase the magnitude of the electric field.

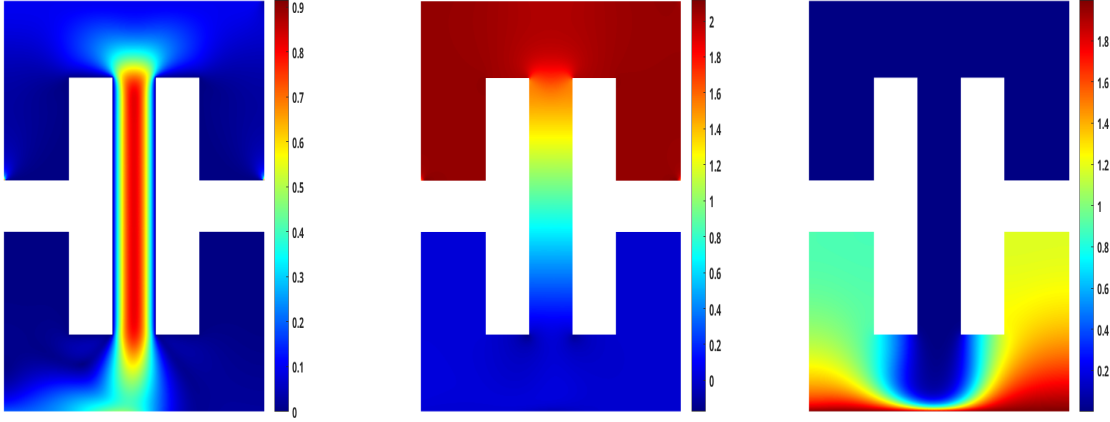


Figure 3: [Example 3] Snapshots of flow dynamics of the electrically charged fluid in a nanosensor: discrete velocity magnitude, pressure, and potential for VEM order $k = 1$ with $\mathbf{E} = [0.1, -0.1]^t$

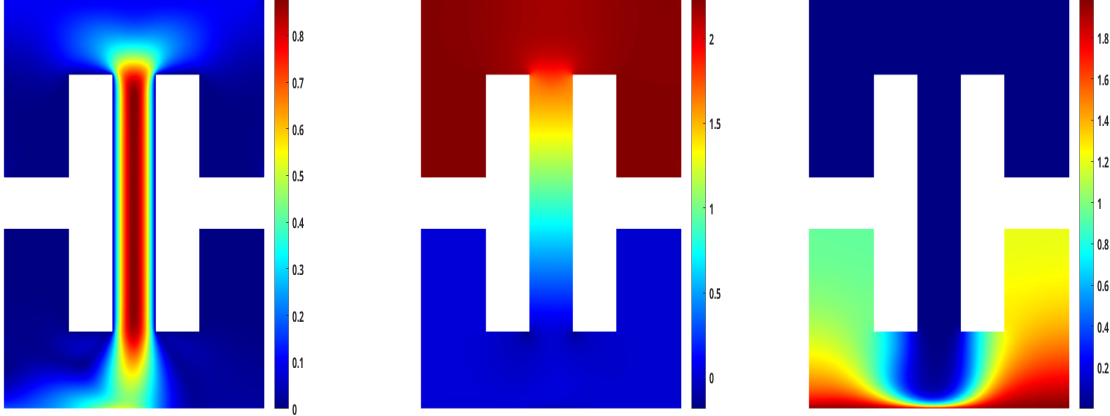


Figure 4: [Example 3] Snapshots of the flow dynamics of the electrically charged fluid in a nanosensor: discrete velocity magnitude, pressure, and potential for VEM order $k = 2$ with $\mathbf{E} = [0.1, -0.1]^t$

Physical interpretation. The flow patterns observed in Figures 3–6 are consistent with well-established electrokinetic transport phenomena in confined geometries. The recirculation zones near the T-shaped obstacles arise from the competition between electro-osmotic slip velocity at charged boundaries and adverse pressure gradients induced by geometric constriction. These recirculation regions are relevant for nanopore sensing applications, as they create zones of extended residence time that can enhance biomolecule capture and detection sensitivity. The slight asymmetry in all fields, caused by the non-axial electric field orientation, influences charged particle trajectories—a mechanism exploitable for biomolecule trajectory control. The VEM formulation successfully

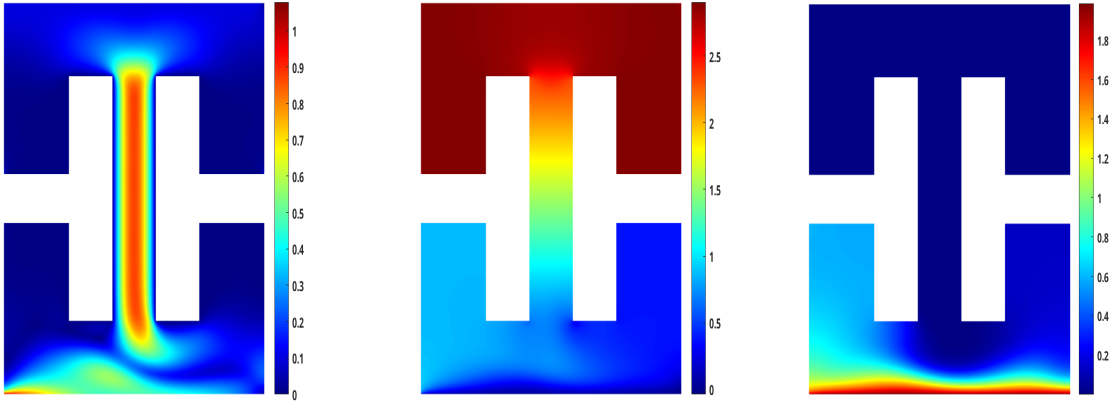


Figure 5: [Example 3] Snapshots of the flow dynamics of the electrically charged fluid in a nanosensor: discrete velocity magnitude, pressure, and potential for VEM order $k = 2$ with $\mathbf{E} = [1, -1]^t$.

Table 5: Comparison of mesh flexibility and geometric capabilities

Feature	Taylor–Hood FEM	Equal-Order VEM
Element types	Triangles only	Arbitrary polygons
Non-convex elements	Not supported	Fully supported
Hanging nodes	Constraint equations	Natural treatment
Mesh distortion tolerance	Moderate (quality-dependent)	High (projection-based)
Adaptive refinement	Transition elements needed	Straightforward
Irregular boundaries	Many small elements	Fewer conforming polygons

captures these characteristic electrokinetic phenomena, e.g., electro-osmotic plug flow in the channel core, boundary-layer-driven recirculation near obstacles, and smooth potential gradients governed by the Poisson–Boltzmann coupling, without requiring specialized mesh treatment for the complex obstacle geometries.

When the field magnitude increases from $\mathbf{E} = [0.1, -0.1]^t$ to $\mathbf{E} = [1, -1]^t$, recirculation intensifies and velocity magnitudes increase proportionally, consistent with the linear electro-osmotic velocity–field relationship in the small Debye–Hückel parameter regime. The curved obstacle configuration produces smoother flow transitions, smaller recirculation zones, and reduced pressure losses compared to sharp T-shaped corners—a geometric effect relevant for applications such as DNA sequencing where consistent translocation velocity is desirable. These results confirm that the proposed VEM formulation captures the essential coupled fluid-electrostatic interactions in realistic nanopore geometries, with the polygonal mesh framework providing natural geometric conformity to the obstacle boundaries without special mesh treatment.

5.4. Comparison with finite element methods

The numerical experiments presented above demonstrate optimal convergence across diverse mesh types and realistic nanopore geometries. We now compare the proposed VEM formulation with the Taylor–Hood finite element approach of AlSohaim et al. [2], which employs $\mathbb{P}_{k+1}/\mathbb{P}_k$ elements on triangular meshes, to highlight the computational and geometric distinctions between the two frameworks.

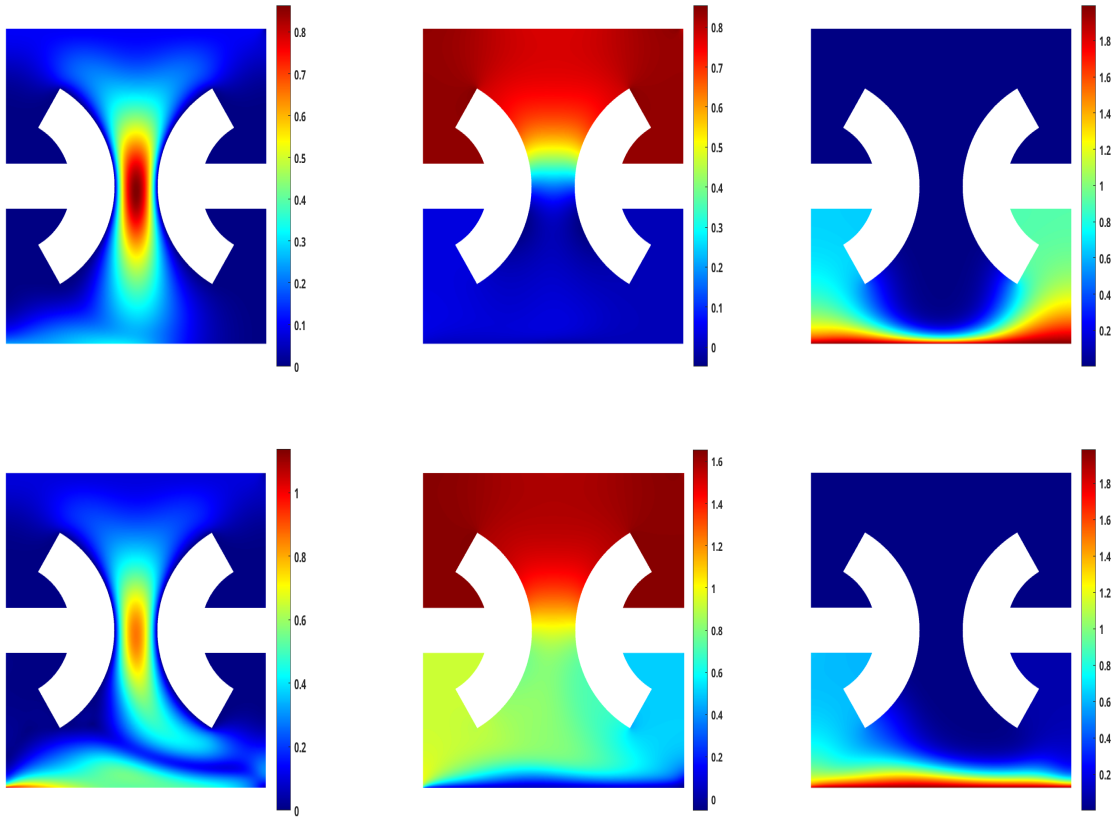


Figure 6: [Example 3] Snapshots of the flow dynamics of the electrically charged fluid in a nanosensor with curved shaped obstacles: discrete velocity magnitude, pressure, and potential for VEM order $k = 2$ with $\mathbf{E} = [0.1, -0.1]^t$ (top) and $\mathbf{E} = [1, -1]^t$ (bottom).

For a polygonal mesh Ω_h with N_v vertices, N_e edges, and N_E elements, the total degrees of freedom for the VEM discretization of order k (accounting for velocity, pressure, and potential, each using the space $V_h(E)$ from Section 3.3) are:

$$\text{DOF}_{\text{VEM}} = 4N_v + 4(k-1)N_e + 4N_E \dim(\mathbb{P}_{k-2}), \quad (5.1)$$

where $\dim(\mathbb{P}_{k-2}) = (k-1)k/2$ for $k \geq 2$ and equals zero for $k = 1$. For Taylor–Hood finite elements on a comparable triangular mesh, the higher-order velocity space \mathbb{P}_{k+1} modifies the count to:

$$\text{DOF}_{\text{FEM}} = 4N_v^{\text{FEM}} + (4k-2)N_e^{\text{FEM}} + N_E^{\text{FEM}}(2\dim(\mathbb{P}_{k-2}) + 2\dim(\mathbb{P}_{k-3})). \quad (5.2)$$

For $k = 1$, VEM requires $4N_v$ DOFs while FEM requires $4N_v + 2N_e$; with typical triangular mesh topology ratios $N_e \approx 1.5 N_v$, this yields a reduction of approximately 43% in total degrees of freedom. For $k = 2$, VEM requires $(4N_v + 4N_e + 4N_E)$ DOFs while FEM requires $(4N_v + 6N_e + 2N_E)$ DOFs; under the additional assumption $N_E \approx 0.5 N_v$, the reduction is approximately 15%. We note that these ratios depend on mesh topology and element counts, and the reduction is more pronounced at lower polynomial orders where the difference in velocity approximation order has a larger relative impact.

The equal-order formulation provides two key structural simplifications relative to mixed finite element methods. First, all three fields, e.g., velocity, pressure, and potential, are approximated

by the same local virtual element space $V_h(E)$ with identical degrees of freedom structure. The projection operators $\Pi_k^{\nabla,E}$ and $\Pi_k^{0,E}$ defined in (3.5)–(3.7) are computed once per element and reused across all field components, eliminating the need for separate shape function implementations, quadrature rules, and local-to-global mappings for different approximation orders. Second, the reformulation of the drag force term $-\epsilon\Delta\psi\mathbf{E}$ using the transport potential equation eliminates second-order derivatives from the momentum residual. Only first-order derivatives $\nabla\psi_h$ appear in the stabilization terms $\mathcal{L}_{1,h}$, $\mathcal{L}_{2,h}$, and $\mathcal{L}_{3,h}$, which are well-defined for functions in the H^1 -conforming space V_h and involve only polynomial projected quantities computable from the degrees of freedom.

Table 5 summarizes the geometric capabilities distinguishing the two frameworks. The VEM framework requires only the mild mesh regularity assumption **(A1)** from Section 3: star-shapedness with respect to a ball of radius $\geq \delta_0 h_E$ and edge length $\geq \delta_0 h_E$. Subject to these constraints, elements may be convex or non-convex, have any number of edges, and accommodate hanging nodes without constraint equations. The convergence studies presented in Examples 5.1–5.2 confirm that optimal $\mathcal{O}(h^k)$ rates are achieved across all these mesh types.

6. Conclusions

We have presented an equal-order virtual element method for the coupled Stokes–Poisson–Boltzmann equations on general polygonal meshes. The formulation employs a $\mathbb{P}_k/\mathbb{P}_k/\mathbb{P}_k$ approximation for velocity, pressure, and potential, stabilized through a residual-based scheme that exploits the structure of the drag force coupling to eliminate second-order derivative terms from the discrete problem. Well-posedness of the continuous and discrete problems was established through the Banach and Brouwer fixed-point theorems, respectively, under explicit smallness conditions on the data, and optimal a priori error estimates of order $\mathcal{O}(h^k)$ were derived in the energy norm. Numerical experiments confirmed these theoretical predictions across diverse mesh types—including non-convex polygons, Voronoi tessellations, distorted elements, and meshes with hanging nodes—and demonstrated the method’s applicability to electro-osmotic flows in nanopore sensors with T-shaped and curved obstacle geometries.

Several directions for future research emerge from this work. The formulation can be extended to the coupled Poisson–Nernst–Planck system to model multiple ionic species and to time-dependent Stokes–Poisson–Boltzmann equations for dynamic electrokinetic phenomena. Development of pressure-robust error estimates, where velocity errors are independent of pressure regularity, represents a natural next step; preliminary investigations using $H(\text{div})$ -conforming velocity reconstructions show promise for extending the pressure-robust framework to the VEM setting, and this work is currently in progress. Extension to polyhedral meshes in three dimensions and incorporation of convective terms through SUPG stabilization for higher Reynolds number regimes would further broaden applicability to realistic engineering configurations.

Acknowledgments

G. Manzini is affiliated to GNCS-INDAM, the Italian Gruppo Nazionale Calcolo Scientifico - Istituto Nazionale di Alta Matematica. AI tools may have served as writing and editing assistants; however, the authors carefully reviewed the manuscript and take full responsibility for the content of this work.

Data Availability

No data was used for the research described in the article.

Declarations

Conflict of interest

The authors declare no conflict of interest during the current study. G. Manzini is also affiliated with Los Alamos National Laboratory. However, this work was carried out entirely outside the scope of any activities, duties, or appointments at Los Alamos National Laboratory or the U.S. Department of Energy. Los Alamos National Laboratory and the U.S. Department of Energy had no role in the conception, execution, funding, or supervision of this work, and assert no rights, title, or interest, including intellectual property rights, in the results presented herein. The views and conclusions expressed are solely those of the authors and do not represent the views of Los Alamos National Laboratory, the U.S. Department of Energy, or their employees or contractors.

Funding

No funding was received by the Authors to prepare this manuscript.

Authors' contribution

All authors equally contributed to this work.

References

- [1] C. Dekker. Solid-state nanopores. *Nature Nanotechnology*, 2:209–215, 2007.
- [2] A. AlSohaim, R. Ruiz-Baier, and S. Villa-Fuentes. Analysis of a finite element method for the Stokes–Poisson–Boltzmann equations. *arXiv preprint arXiv:2502.06455*, 2025.
- [3] R. F. Probstein. *Physicochemical Hydrodynamics: An Introduction*. Wiley-Interscience, New York, 2nd edition, 1994.
- [4] B. J. Kirby. *Micro-and nanoscale fluid mechanics: transport in microfluidic devices*. Cambridge university press, 2010.
- [5] J. H. Masliyah and S. Bhattacharjee. *Electrokinetic and Colloid Transport Phenomena*. Wiley-Interscience, 2006.
- [6] P. M. Biesheuvel and M. Z. Bazant. Nonlinear dynamics of capacitive charging and desalination by porous electrodes. *Physical Review E*, 81(3):031502, 2010.
- [7] G. M. Whitesides. The origins and the future of microfluidics. *Nature*, 442:368–373, 2006.
- [8] L. Chen, M. Holst, and J. Xu. The finite element approximation of the nonlinear Poisson–Boltzmann equation. *SIAM J. Numer. Anal.*, 45(6):2298–2320, 2007.
- [9] J. Kraus, S. Nakov, and S. Repin. Reliable numerical solution of a class of nonlinear elliptic problems generated by the Poisson–Boltzmann equation. *Comput. Methods Appl. Math.*, 20(2):293–319, 2020.

- [10] M. Holst, J. Mccammon, Z. Yu, Y. Zhou, and Y. Zhu. Adaptive finite element modeling techniques for the Poisson-Boltzmann equation. *Commun. Comput. Phys.*, 11(1):179–214, 2012.
- [11] H. Linghan, S. Shi, and Y. Ying. Error analysis of virtual element method for the Poisson–Boltzmann equation. *J. Numer. Math.*, 33(2):187–210, 2025.
- [12] L. Beirao Da Veiga, F. Brezzi, A. Cangiani, G. Manzini, L. Marini, and A. Russo. Basic principles of Virtual Element Methods. *Math. Models Methods Appl. Sci.*, 23:199–214, 2013.
- [13] L. Beirao Da Veiga, F. Brezzi, and L. Marini. Virtual elements for linear elasticity problems. *SIAM J. Numer. Anal.*, 51:794–812, 2013.
- [14] A. Gain, C. Talischi, and G. Paulino. On the virtual element method for three-dimensional linear elasticity problems on arbitrary polyhedral meshes. *Comput. Methods Appl. Mech. Eng.*, 282:132–160, 2014.
- [15] D. Adak, G. Manzini, and S. Natarajan. Nonconforming virtual element methods for velocity-pressure Stokes eigenvalue problem. *Appl. Numer. Math.*, 202:42–66, 2024.
- [16] L. B. Da Veiga, F. Dassi, and G. Vacca. Vorticity-stabilized virtual elements for the Oseen equation. *Math. Models Methods Appl. Sci.*, 31(14):3009–3052, 2021.
- [17] L. B. Da Veiga, C. Lovadina, and G. Vacca. Virtual elements for the Navier-Stokes problem on polygonal meshes. *SIAM J. Numer. Anal.*, 56(3):1210–1242, 2018.
- [18] L. B. Da Veiga, C. Lovadina, and G. Vacca. Divergence free virtual elements for the Stokes problem on polygonal meshes. *ESAIM: Math. Model. Numer. Anal.*, 51(2):509–535, 2017.
- [19] G. Vacca. An H^1 -conforming virtual element for Darcy and Brinkman equations. *Math. Models Methods Appl. Sci.*, 28(01):159–194, 2018.
- [20] P. Antonietti, G. Vacca, and M. Verani. Virtual element method for the Navier-Stokes equation coupled with the heat equation. *IMA J. Numer. Anal.*, pages 1–34, 11 2022.
- [21] D. Adak, D. Mora, S. Natarajan, and A. Silgado. A virtual element discretization for the time dependent Navier–Stokes equations in stream-function formulation. *ESAIM: Math. Model. Numer. Anal.*, 55(5):2535–2566, 2021.
- [22] S. Mishra, E. Natarajan, and S. Natarajan. A SUPG-stabilized virtual element method for the Navier–Stokes equation: approximations of branches of non-singular solutions. *Adv. Comput. Math.*, 51(4):34, 2025.
- [23] L. da Veiga, F. Dassi, G. Manzini, and L. Mascotto. Virtual elements for Maxwell’s equations. *Computers & Mathematics with Applications*, 116:82–99, 2022.
- [24] F. Brezzi and L. Marini. Virtual element methods for plate bending problems. *Comput. Methods Appl. Mech. Eng.*, 253:455–462, 2013.
- [25] F. Aldakheel, B. Hudobivnik, A. Hussein, and P. Wriggers. Phase-field modeling of brittle fracture using an efficient virtual element scheme. *Comput. Methods Appl. Mech. Eng.*, 341:443–466, 2018.

[26] M. Benedetto, A. Caggiano, and G. Etse. Virtual elements and zero thickness interface-based approach for fracture analysis of heterogeneous materials. *Comput. Methods Appl. Mech. Eng.*, 338:41–67, 2018.

[27] P. Antonietti, M. Bruggi, S. Scacchi, and M. Verani. On the virtual element method for topology optimization on polygonal meshes: A numerical study. *Comput. Math. Appl.*, 74(5):1091–1109, 2017.

[28] H. Chi, A. Pereira, I. Menezes, and G. Paulino. Virtual element method (VEM)-based topology optimization: an integrated framework. *Struct. Multidiscip. Optim.*, 62(3):1089–1114, 2020.

[29] L. Beirao Da Veiga, F. Brezzi, F. Dassi, L. Marini, and A. Russo. Virtual element approximation of 2d magnetostatic problems. *Comput. Meth. Appl. Mech. Engrg.*, 327:173–195, 2017.

[30] J. Guo and M. Feng. A new projection-based stabilized virtual element method for the Stokes problem. *J. Sci. Comput.*, 85(1):16, 2020.

[31] D. Irisarri and G. Hauke. Stabilized virtual element methods for the unsteady incompressible Navier-Stokes equations. *Calcolo*, 56(4):38, 2019.

[32] Y. Li, M. Feng, and Y. Luo. A new local projection stabilization virtual element method for the Oseen problem on polygonal meshes. *Adv. Comput. Math.*, 48(3):30, 2022.

[33] S. Mishra and E. Natarajan. A unified local projection-based stabilized virtual element method for the coupled Stokes–Darcy problem. *Adv. Comput. Math.*, 50(6):106, 2024.

[34] S. Mishra and E. Natarajan. An equal-order virtual element framework for the coupled Stokes–Temperature equation with nonlinear viscosity. *J. Sci. Comput.*, 104(2):73, 2025.

[35] V. Girault and P. Raviart. *Finite Element Methods for Navier-Stokes Equations. Theory and Algorithm*. Springer-Verlag, Berlin Heidelberg NewYork, 1986.

[36] L. Beirao Da Veiga, F. Brezzi, L. Marini, and A. Russo. Virtual element method for general second-order elliptic problems on polygonal meshes. *Math. Models Methods Appl. Sci.*, 26(04):729–750, 2016.

[37] B. Ahmad, A. Alsaedi, F. Brezzi, L. Marini, and A. Russo. Equivalent projectors for virtual element methods. *Comput. Math. Appl.*, 66(3):376–391, 2013.

[38] S. Brenner and L. Scott. *The Mathematical Theory of Finite Element Methods*. 3rd ed., Springer, New York, 2008.

[39] A. Cangiani, E. Georgoulis, T. Pryer, and O. Sutton. A posteriori error estimates for the virtual element method. *Numer. Math.*, 137:857–892, 2018.

[40] L. Chen and J. Huang. Some error analysis on virtual element methods. *Calcolo*, 55, 2017.

[41] S. Mishra and E. Natarajan. Local projection stabilization virtual element method for the convection-diffusion equation with nonlinear reaction term. *Comput. Math. Appl.*, 152:181–198, 2023.

[42] G. Mitscha-Baude, A. Buttinger-Kreuzhuber, G. Tulzer, and C. Heitzinger. Adaptive and iterative methods for simulations of nanopores with the PNP–Stokes equations. *J. Comput. Phys.*, 338:452–476, 2017.